[redacted]

Copy 6
RM L56A24

C, 2

NACA

RESEARCH MEMORANDUM

INVESTIGATION AT HIGH SUBSONIC SPEEDS OF SOME EFFECTS OF SIDESLIP ON THE AERODYNAMIC LOADS ON FINNED AND UNFINNED BODIES MOUNTED FROM THE WING OF A SWEPT-WING—FUSELAGE MODEL

By Thomas J. King, Jr.

Langley Aeronautical Laboratory
Langley Field, Va.

CLASSIFICATION CHANGED TO UNCLASSIFIED

By authority of NACA Res Abs RN-124 Date Jan. 29, 1958

AMT 2-18-58

CLASSIFIED DOCUMENT

This material contains information affecting the National Defense of the United States within the meaning of the espionage laws, Title 18, U.S.C., Secs. 793 and 794, the transmission or revelation of which in any manner to an unauthorized person is prohibited by law.

NATIONAL ADVISORY COMMITTEE FOR AERONAUTICS

WASHINGTON
April 26, 1956

[redacted]

NASA Technical Library
3 1176 01437 7668

NACA RM L56A24

NATIONAL ADVISORY COMMITTEE FOR AERONAUTICS

RESEARCH MEMORANDUM

INVESTIGATION AT HIGH SUBSONIC SPEEDS OF SOME EFFECTS OF SIDESLIP ON THE AERODYNAMIC LOADS ON FINNED AND UNFINNED BODIES MOUNTED FROM THE WING OF A SWEPT-WING—FUSELAGE MODEL

By Thomas J. King, Jr.

SUMMARY

An investigation has been made in the Langley high-speed 7- by 10-foot tunnel at Mach numbers from 0.50 to 0.94 to determine the aerodynamic loads on finned and unfinned bodies in the presence of a swept wing. A tip-mounted body at 1.04 semispan and an underwing pylon-mounted body at 0.33 semispan were investigated.

The normal force and yawing moment of a tip-mounted body (fins off) varied considerably with the angle of sideslip at moderate and high angles of attack. Adding fins to the body generally increased the normal force, the rolling moment, and the slope of the side-force curve, decreased the nose-up pitching moments, and reversed the unstable variation of the yawing moment. The trends indicated at a Mach number of 0.50 and an angle of attack of 0° were fairly representative of the results at Mach numbers from 0.50 to 0.94, although at the higher angles of attack some significant quantitative effects of Mach number were noted.

INTRODUCTION

The National Advisory Committee for Aeronautics is conducting investigations of nacelles and external stores for use on high-speed aircraft. One phase of these investigations has been the evaluation of the aerodynamic loads on externally mounted nacelles and stores. Results at subsonic speeds of investigations of wing-fuselage models at zero sideslip conditions with bodies mounted from the wings are presented in references 1 to 4. Loads on external stores on a swept-wing fighter-type airplane during maneuvering flight at subsonic speeds are presented in reference 5. The present paper presents the aerodynamic loading

characteristics at subsonic speeds of finned and unfinned bodies mounted from a swept wing at sideslip conditions for various angles of attack.

The results presented herein were obtained in the Langley high-speed 7- by 10-foot tunnel at Mach numbers from 0.50 to 0.94 at various angles of attack over an angle-of-sideslip range which was dependent upon the limiting loads of the body strain-gage balance.

SYMBOLS

The system of axes used for the body, with positive forces, moments, and angles indicated, is presented in figure 1. The coefficients and symbols used in this paper are defined as follows:

$F_{N,b}$	body normal force, lb
$M_{Y,b}$	body pitching moment, tip position - referred to $0.547l$, inboard position - referred to $0.462l$, ft-lb
$M_{X,b}$	body rolling moment, ft-lb
$M_{Z,b}$	body yawing moment, tip position - referred to $0.547l$, inboard position - referred to $0.462l$, ft-lb
$F_{Y,b}$	body side force, lb
$C_{N,b}$	body normal-force coefficient, $\frac{F_{N,b}}{qA}$
$C_{m,b}$	body pitching-moment coefficient, $\frac{M_{Y,b}}{qAl}$
$C_{l,b}$	body rolling-moment coefficient, $\frac{M_{X,b}}{qAl}$
$C_{n,b}$	body yawing-moment coefficient, $\frac{M_{Z,b}}{qAl}$
$C_{Y,b}$	body side-force coefficient, $\frac{F_{Y,b}}{qA}$
C_L	wing-fuselage lift coefficient, $\frac{\text{Lift}}{qS}$
q	free-stream dynamic pressure, lb/sq ft

[redacted]

R	Reynolds number based on $\bar{c}$
S	wing area, sq ft
A	maximum frontal area of body, sq ft
$\bar{c}$	mean aerodynamic chord of wing, $\frac{2}{S}\int_0^{b/2} c^2 dy$ (using theoretical tip), ft
c	local wing chord, ft
c_p	pylon chord, ft
b	wing span, ft
l	body length, ft
l_f	fuselage length, ft
d	body diameter, ft
d_f	fuselage diameter, ft
y	spanwise distance from plane of symmetry of wing-fuselage model, ft
z	vertical distance from wing chord plane to body center line, ft
M	Mach number
α	angle of attack, deg
β	angle of sideslip, deg

Subscript:

max	maximum

MODELS AND APPARATUS

A drawing of the wing, fuselage, and bodies used in this investigation is presented in figure 2. The aluminum-alloy wing had an aspect ratio of 4.0, taper ratio of 0.6, sweep of 46.7°, and NACA 65A006 airfoil sections parallel to the fuselage center line.

The fuselage was constructed of aluminum alloy and was formed by parabolic arc segments, the ordinates for which are given in table I. The bodies were generated by revolution of a profile made up of ogival nose and tail sections, between which was located a straight midsection. Ordinates of the body, which had a fineness ratio of 9.34, are presented in table II.

The pylons, ordinates for which are presented in table III, were unswept and untapered and had flat sides. Details of the body fins are shown in figure 3. The fins were oriented at 45° from the vertical and horizontal.

The wing-fuselage model was attached to the supporting sting by an internal strain-gage balance. The model forces were measured by the balance and were recorded automatically.

The body was instrumented with a five-component balance and was mounted from the left wing in each of the two positions shown in figure 2. The configuration with the body mounted from the pylon had a wooden body symmetrically mounted from the right wing. The configuration with the wing-tip-mounted body had only the instrumented body on the left wing tip. A cutaway drawing showing the installation of the balance on the wing tip and pylon is presented in figure 4. The body housing the balance was constructed of plastic reinforced with fiberglass cloth. In the inboard position, the moment axes of the body were located 8.56 inches from the body nose; in the tip position, the moment axes were 10.14 inches from the body nose.

TESTS AND RESULTS

The tests were conducted in the Langley high-speed 7- by 10-foot tunnel. Body loads were obtained for the tip-mounted body through a Mach number range that usually extended from 0.50 to 0.94. This configuration was tested over an angle-of-sideslip range at angles of attack of approximately 0°, 6.5°, and 13.0°. The angle-of-sideslip range was restricted by the load limits of the body balance and therefore varied with angle of attack and Mach number.

Because of difficulties experienced with the body-loads balance, tests of the pylon-mounted finned body were completed only for an angle of attack of approximately 6.5° and Mach numbers of 0.50 and 0.70.

The aerodynamic characteristics of the bodies in the presence of the model are given as body normal-force, side-force, rolling-moment, yawing-moment, and pitching-moment coefficients plotted against angle of sideslip at constant angle of attack. These force and moment results

are presented relative to the system of body axes as shown in figure 1. The body force coefficients are based on the maximum frontal area of the body; body moment coefficients are based on the maximum frontal area and length of the body.

The body coefficients are the forces and moments of the body in the presence of the wing, fuselage, and pylon, and hence include the interference of these parts on the body.

The variation with Mach number of the Reynolds number based on wing mean aerodynamic chord is shown in figure 5.

CORRECTIONS

Blocking corrections applied to Mach number and dynamic pressure were determined by the velocity-ratio method of reference 6, which utilizes experimental pressures measured at the tunnel wall opposite the model. The correction to Mach number increased with speed and at $M = 0.94$ was 0.01.

The jet-boundary corrections applied to the angle of attack were calculated by the method of reference 7.

Corrections have been applied to the angle of sideslip and angle of attack to account for deflection of the sting-support system under load. No correction has, however, been applied to the results to account for aeroelastic distortion of the wing.

DISCUSSION

The body loading characteristics of the finned and unfinned tip-mounted body are presented in figures 6 to 8. The body loading characteristics of the finned pylon-mounted body at $\alpha \approx 6.5^{\circ}$ are presented in figure 9. The tip-mounted body results at a Mach number of 0.50 are summarized in figure 10.

In interpreting the body forces and moments it should be kept in mind that the measurements were made on the left wing of the model and that the lines of action of the forces and moments are as indicated in figure 1.

Large changes in the tip-mounted body forces and moments resulted from changes in angle of attack and sideslip and from addition of the fins. At zero angle of attack the unfinned-body forces and moments,

[redacted]

with the exception of the yawing moments, were little affected by changes in angle of sideslip (fig. 10(a)); however, adding the fins to the body increased the slope of the side-force curve and reversed the unstable variation of the yawing moment (fig. 10(b)).

As has been indicated by the angle-of-attack tests of reference 4, increasing the angle of attack produced considerable variation in the body loads, particularly the normal force and yawing moment, over the sideslip-angle range. Adding fins to the body generally increased the normal force, the rolling moment, and the slope of the side-force curve, decreased the nose-up pitching moments, and reversed the unstable variation of the yawing moment (fig. 10(b)).

Although at the high Mach numbers and high angles of attack the data ranges are very limited, the trends indicated at a Mach number of 0.50 and $\alpha = 0^\circ$ were fairly representative of the results at Mach numbers from 0.50 to 0.94. Some quantitative differences due to Mach number are evident (figs. 7 and 8), however, particularly at the high angles of attack.

The results for the inboard pylon-mounted body (fins on) at $\alpha \approx 6.5^\circ$ (fig. 9) show considerable variation of the body lateral components, particularly rolling moment, with change in angle of sideslip. A comparison of the body loads at $M = 0.50$ of the finned tip-mounted and pylon-mounted bodies is presented in figure 11. The tip-mounted body pitching-moment and yawing-moment coefficients have been transferred to 0.4621 for comparison with the pylon-mounted-body coefficients.

In order to illustrate the magnitudes of body forces and moments on a full-size airplane, figure 12 has been prepared. The loads on a tip-mounted body are presented for a sideslip angle of 8° and an altitude of 40,000 feet. The geometry of the assumed airplane is presented in table IV.

At $\alpha = 0^\circ$ the body side forces were larger than the normal forces, and body yawing moments were greater than the pitching and rolling moments (fig. 12). Increases in angle of attack generally increased the body loads. For example, all loads were increased when the angle of attack was changed from 0° to approximately 6.5°. However, at an angle of attack of approximately 13° there were some reductions in all moments. Adding the fins to the body produced large changes in the body loads, particularly the side forces and yawing moments. For example, at $M = 0.80$ and $\alpha \approx 6.5^\circ$ the finned body had a side force of about 800 pounds and yawing moment of about 2200 foot-pounds (nose in) compared to an unfinned-body side force of approximately 350 pounds and yawing moment of 1000 foot-pounds (nose out). (See fig. 12.)

CONCLUSIONS

An investigation at high subsonic speeds of effects of sideslip on the aerodynamic loads on finned and unfinned bodies mounted from the wing of a swept-wing—fuselage model indicates the following conclusions:

1. Normal force and yawing moment of a tip-mounted body (fins off) varied considerably with angle of sideslip at moderate and high angles of attack. Adding fins to the body generally increased the normal force, the rolling moment, and the slope of the side-force curve, decreased the nose-up pitching moments, and reversed the unstable variation of the yawing moment.

2. The trends indicated at an angle of attack of 0° and a Mach number of 0.50 were fairly representative of the range from 0.50 to 0.94 Mach number, although at the higher angles of attack some significant quantitative effects of Mach number were noted.

Langley Aeronautical Laboratory,
National Advisory Committee for Aeronautics,
Langley Field, Va., January 9, 1956.

[redacted]

REFERENCES

1. Silvers, H. Norman, and King, Thomas J., Jr.: Investigation at High Subsonic Speeds of Bodies Mounted From the Wing of an Unswept-Wing—Fuselage Model, Including Measurements of Body Loads. NACA RM L52J08, 1952.

2. Silvers, H. Norman, and O'Bryan, Thomas C.: Some Notes on the Aerodynamic Loads Associated With External-Store Installations. NACA RM L53E06a, 1953.

3. Silvers, H. Norman, King, Thomas J., Jr., and Alford, William J., Jr.: Wind-Tunnel Investigation at High Subsonic Speeds of the Effects of Wing-Mounted External Stores on the Loading and Aerodynamic Characteristics in Pitch of a 45° Sweptback Wing Combined With a Fuselage. NACA RM L54A21, 1954.

4. Alford, William J., Jr., and Silvers, H. Norman: Investigation at High Subsonic Speeds of Finned and Unfinned Bodies Mounted at Various Locations From the Wings of Unswept- and Swept-Wing—Fuselage Models, Including Measurements of Body Loads. NACA RM L54B18, 1954.

5. Hamer, Harold A., and O'Bryan, Thomas C.: Flight Measurements of the Loads and Moments on an External Store Mounted Under the Wing of a Swept-Wing Fighter-Type Airplane During Yawing and Rolling Maneuvers. NACA RM L55G22, 1955.

6. Hensel, Rudolf W.: Rectangular-Wind-Tunnel Blocking Corrections Using the Velocity-Ratio Method. NACA TN 2372, 1951.

7. Gillis, Clarence L., Polhamus, Edward C., and Gray, Joseph L., Jr.: Charts for Determining Jet-Boundary Corrections for Complete Models in 7- by 10-Foot Closed Rectangular Wind Tunnels. NACA WR L-123, 1945. (Formerly NACA ARR L5G31.)

[redacted]

TABLE I.- FUSELAGE ORDINATES

[Basic fineness ratio 12, actual fineness ratio 9.8 achieved by cutting off rear portion of fuselage]

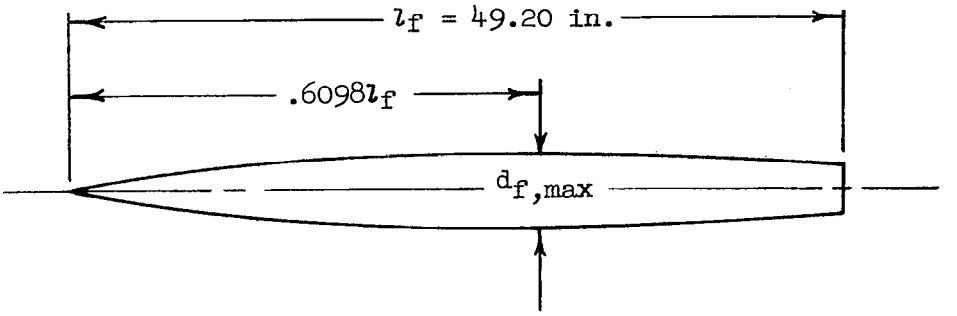

Ordinates, percent length	
Station	Radius
0	0
.61	.28
.91	.36
1.52	.52
3.05	.88
6.10	1.47
9.15	1.97
12.20	2.40
18.29	3.16
24.39	3.77
30.49	4.23
36.59	4.56
42.68	4.80
48.78	4.95
54.88	5.05
60.98	5.08
67.07	5.04
73.17	4.91
79.27	4.69
85.37	4.34
91.46	3.81
100.00	3.35
L. E. radius = 0.0006l_f	

[redacted]

TABLE II.- BODY ORDINATES

[Fineness ratio 9.34]

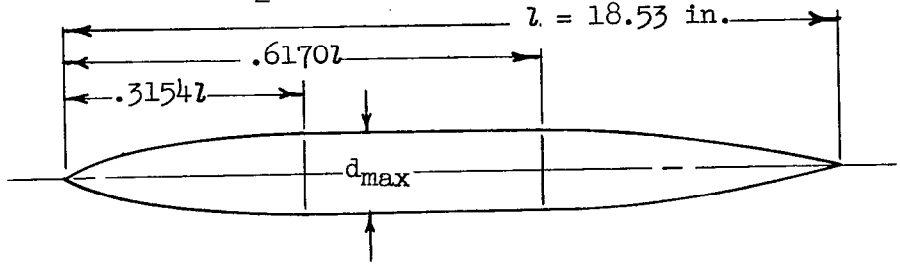

Ordinates, percent length	
Station	Radius
0	0
.36	.30
1.21	.73
3.04	1.44
4.87	2.09
6.71	2.65
8.26	3.07
9.15	3.29
9.69	3.44
10.84	3.70
11.99	3.94
13.14	4.12
14.29	4.30
15.44	4.44
17.74	4.70
20.04	4.92
22.34	5.08
24.64	5.20
26.94	5.30
29.24	5.34
31.54	5.36
61.70	5.36
68.69	5.20
74.95	4.76
81.22	3.94
87.48	2.76
90.60	2.11
93.75	1.42
96.89	.72
98.44	.36
100.00	0

[redacted]

TABLE III.- FLAT-PYLON ORDINATES

[Basic thickness ratio 6.0 percent; actual thickness ratio 6.2 percent, based on actual chord length of 6.14 inches]

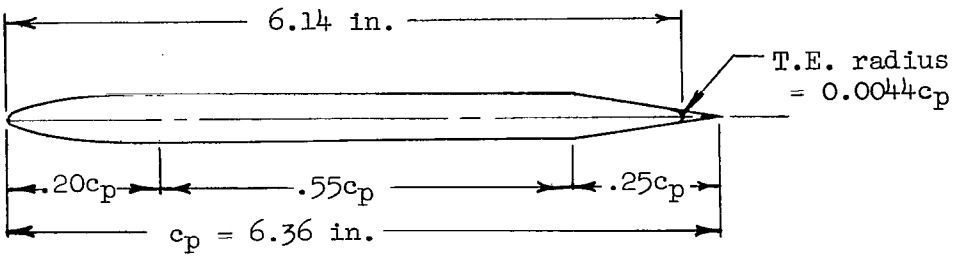

Ordinates, percent chord	
Station	Ordinate
0	0
2.5	.46
5.0	2.00
15.0	2.90
20.0	3.00
75.0	3.00
Straight taper	
100.0	0

TABLE IV.- GEOMETRY OF MODEL AND HYPOTHETICAL AIRPLANE

	Model	Hypothetical airplane
Wing:		
S, sq ft	2.25	324
b, ft	3.00	36
$\bar{c}$, ft	0.765	9.18
Body:		
A, sq ft	0.0215	3.096
l, ft	1.544	18.53

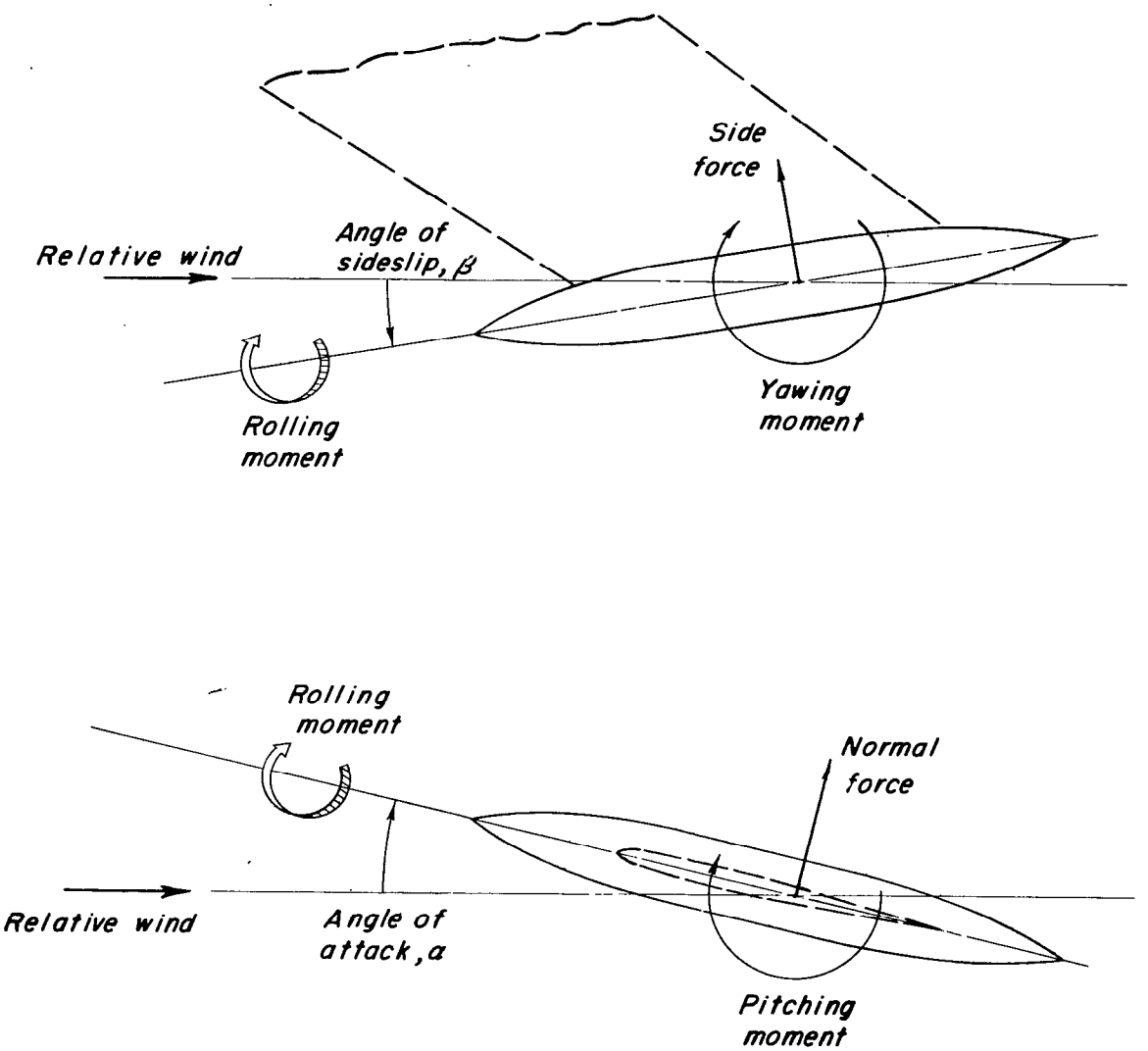

Figure 1.- Positive directions of body forces, moments, and angles.

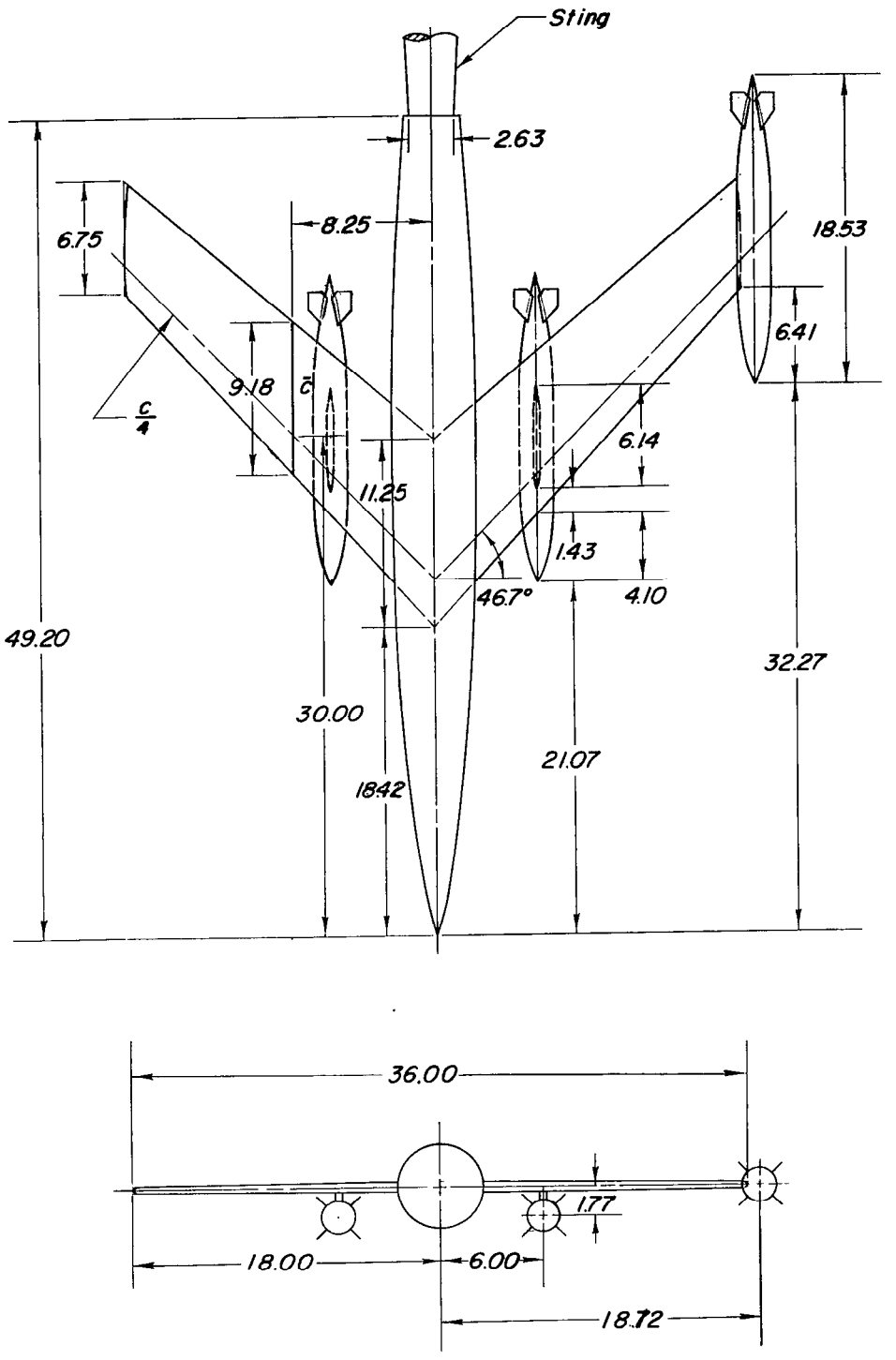

Figure 2.- Drawing of wing, fuselage, and bodies showing tip and inboard locations of the bodies as tested on the sting support system in the Langley high-speed 7- by 10-foot tunnel. All dimensions are in inches.

[redacted]

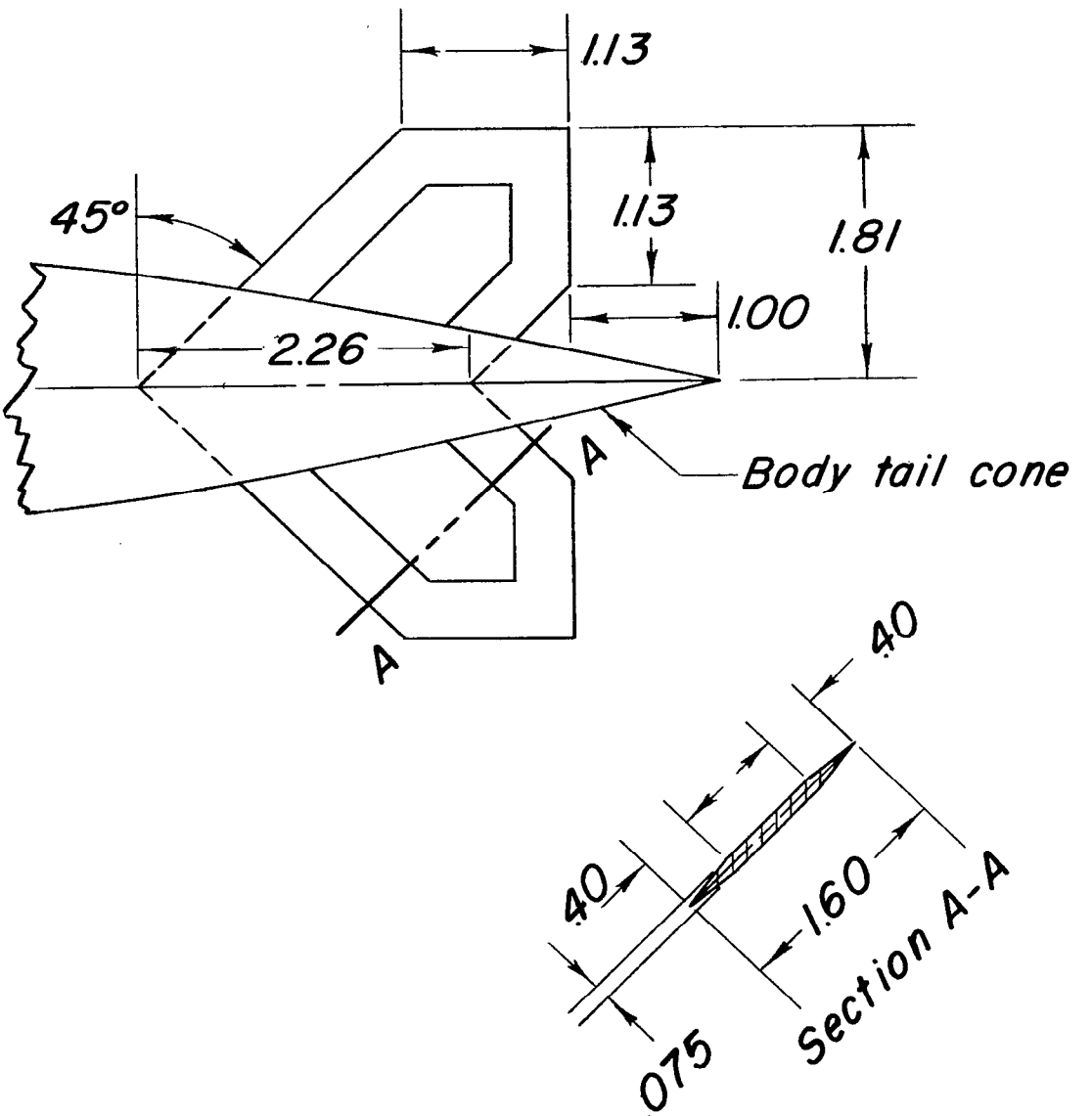

Figure 3.- Details of stabilizing fins. All dimensions are in inches.

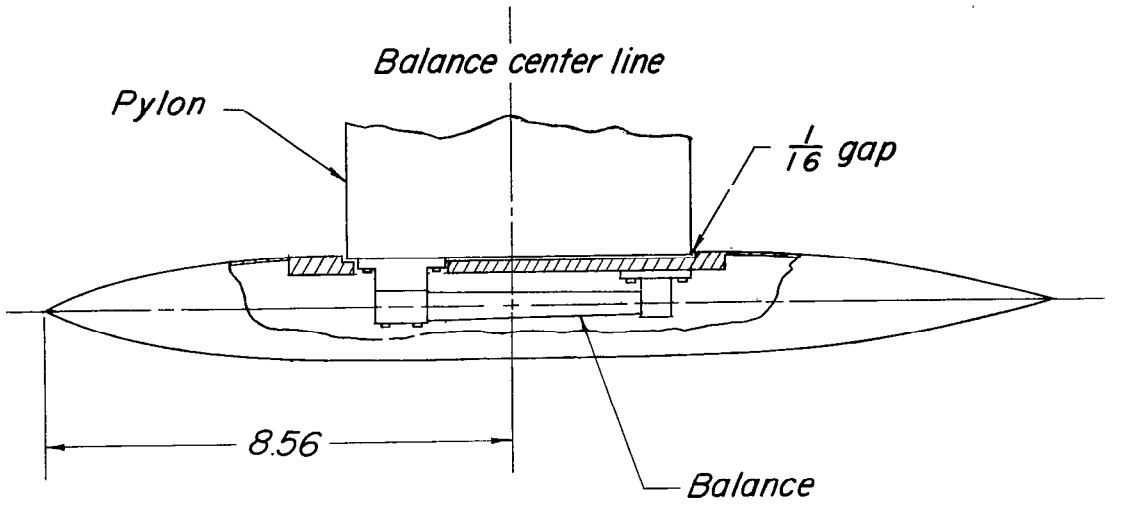

Pylon mounted

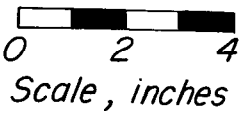

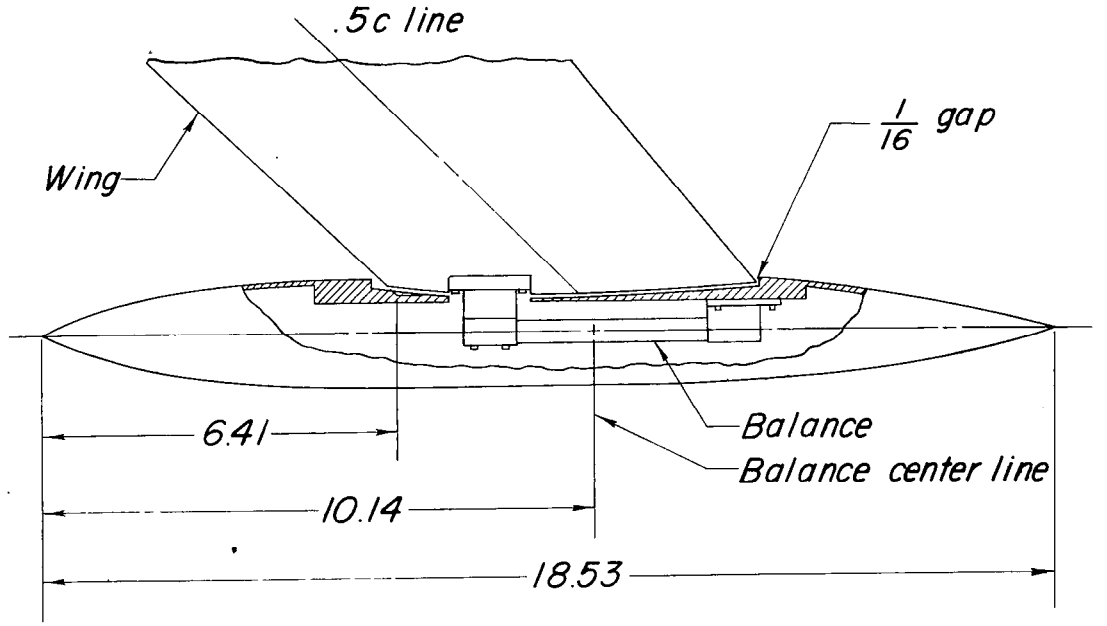

Wing-tip mounted

Figure 4.- Cutaway drawing showing instrumented body as mounted on pylon and on wing tip. All dimensions are in inches.

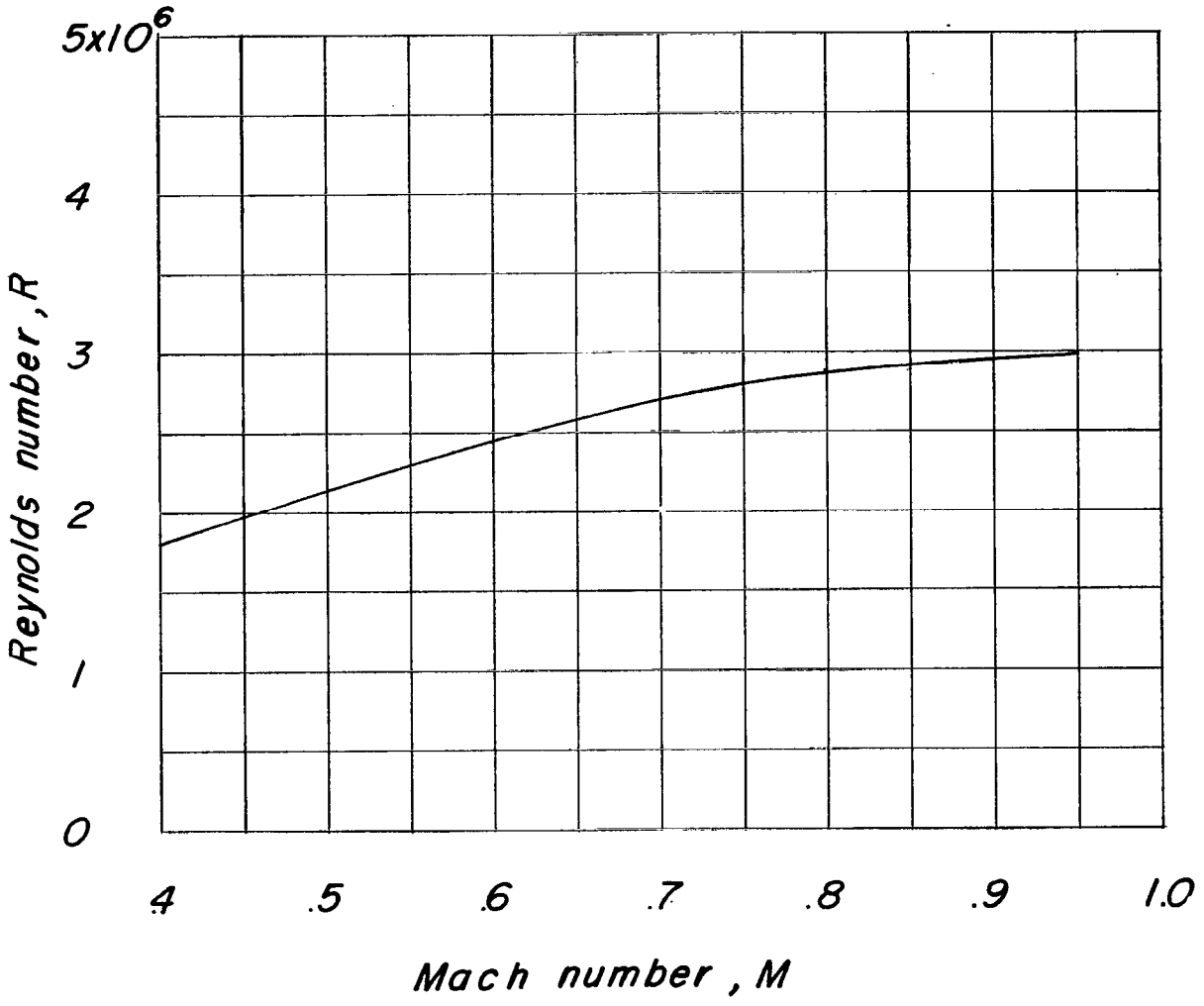

Figure 5.- Variation of average Reynolds number with Mach number. Reynolds number based on wing mean aerodynamic chord (0.765 foot).

[redacted]

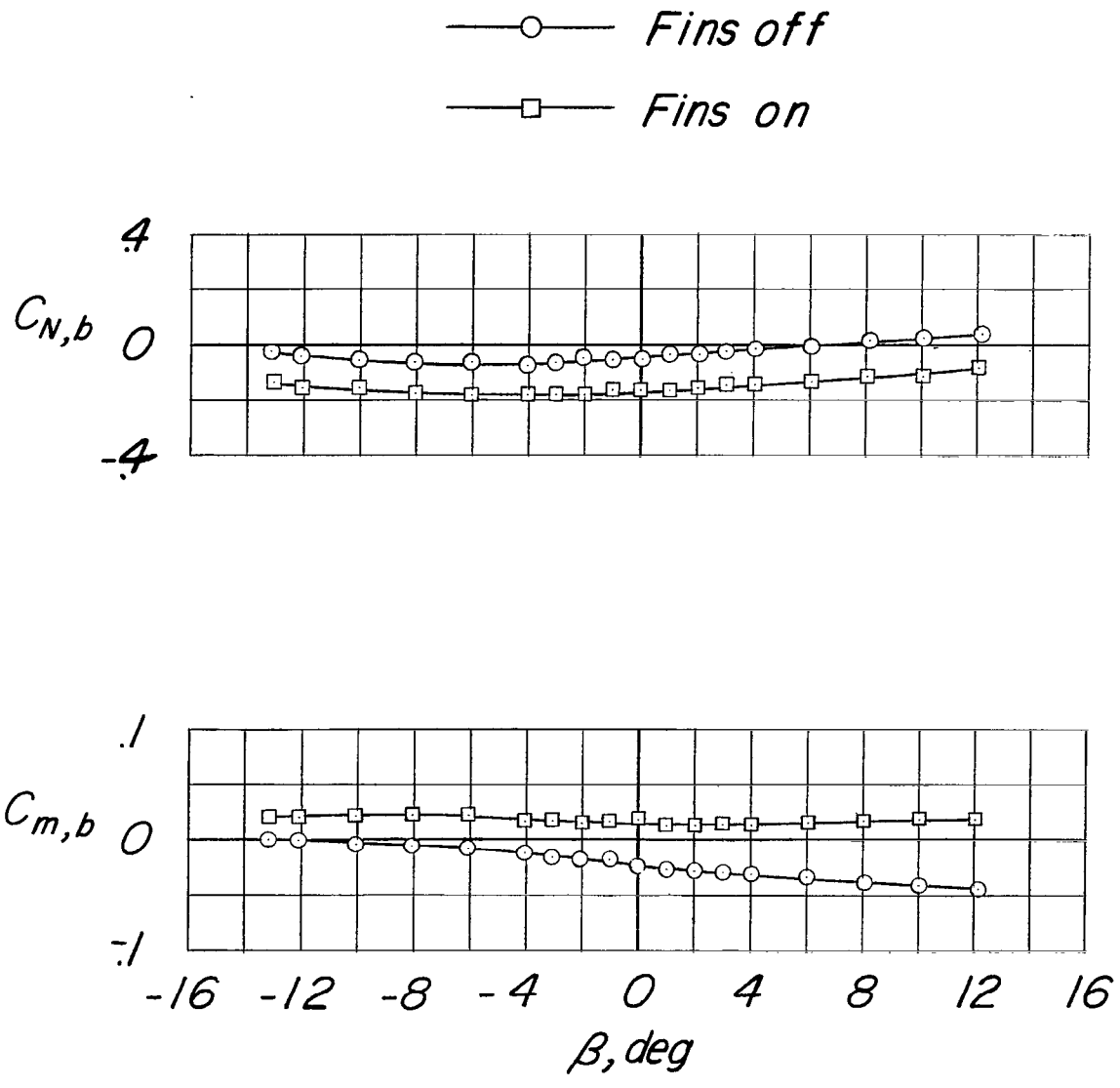

(a) M = 0.50; $\alpha = 0^{\circ}$; $C_L = -0.011$.

Figure 6.- Aerodynamic characteristics of the body mounted on the left wing tip of the swept-wing—fuselage model.

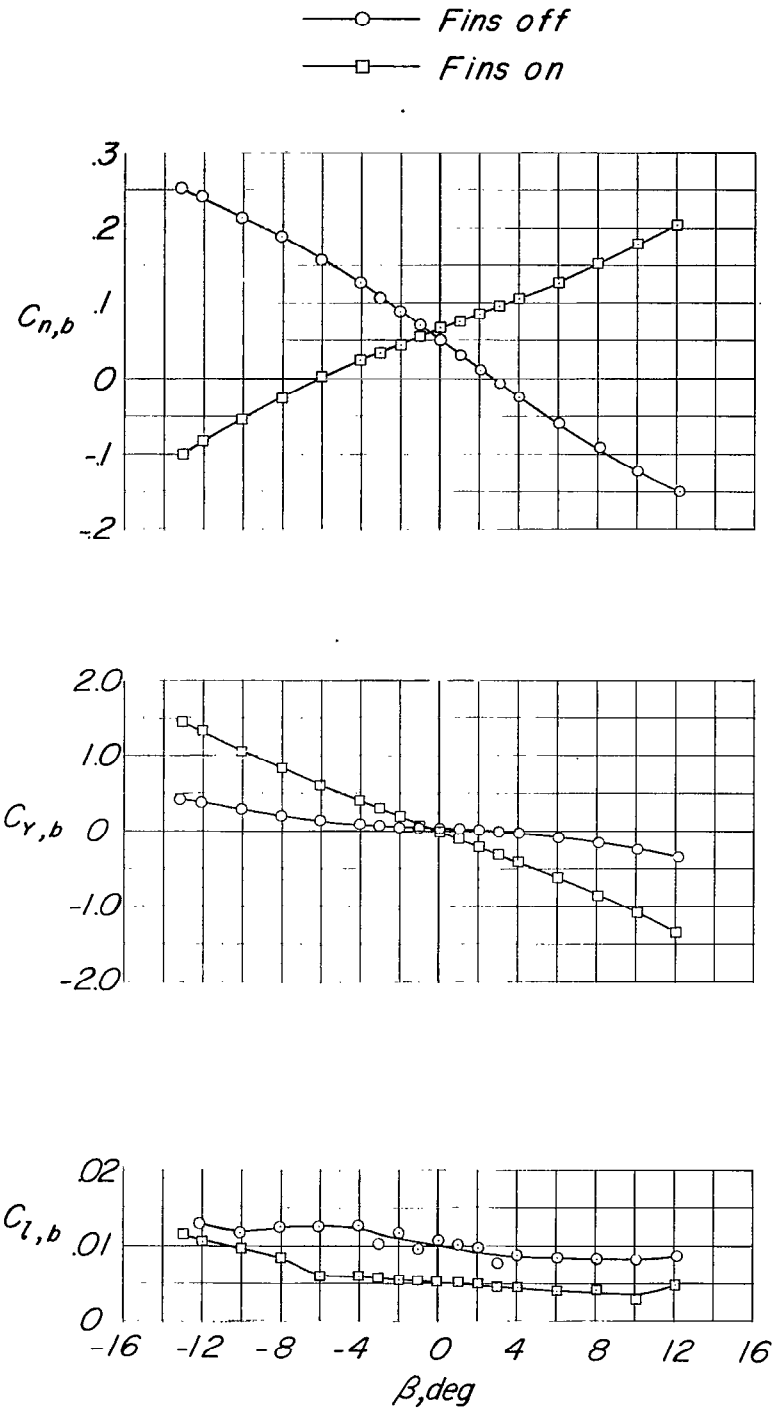

(a) Concluded.

Figure 6.- Continued.

[redacted]

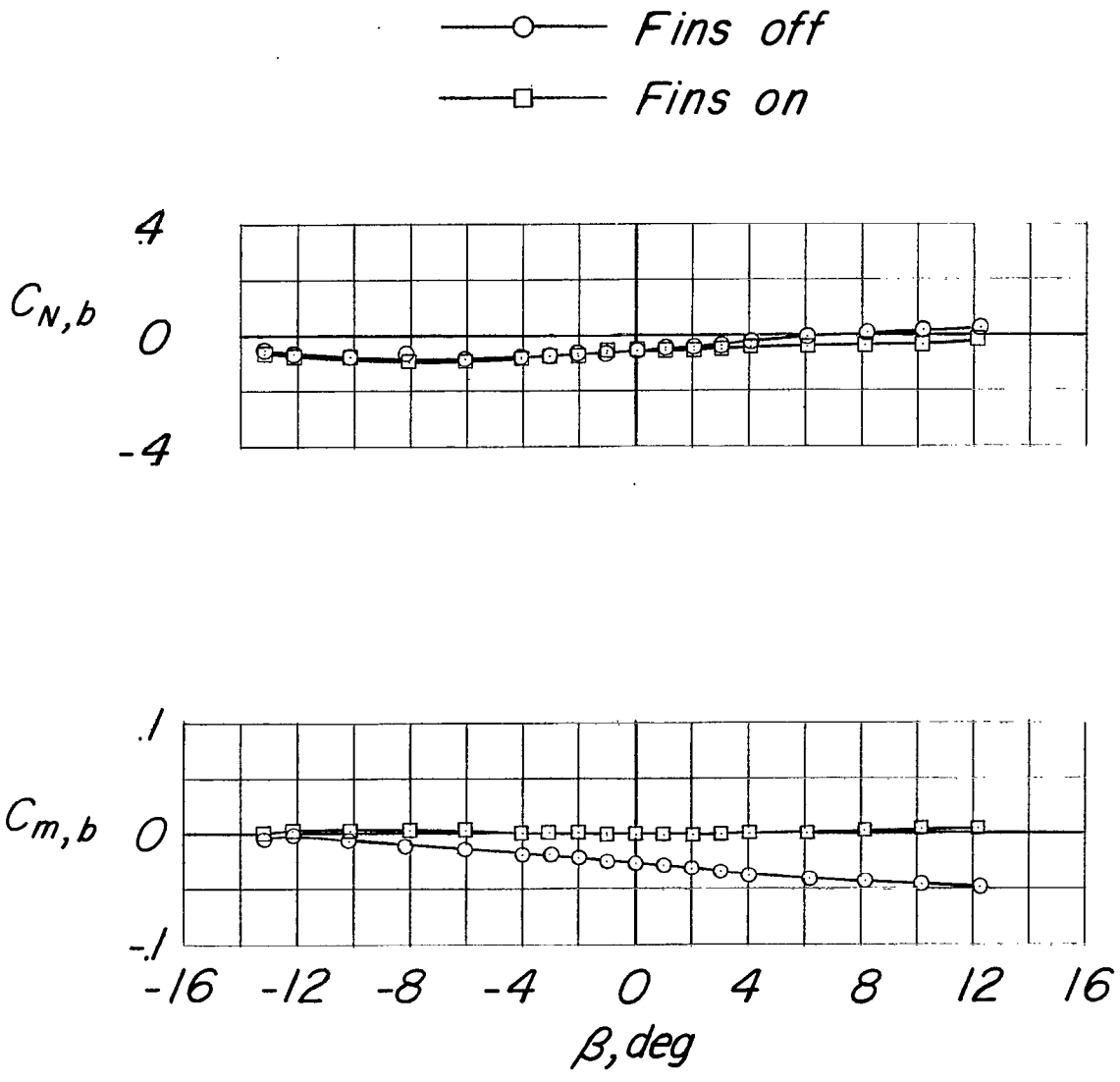

(b) M = 0.70; $\alpha = 0^{\circ}$; $C_L = -0.011$.

Figure 6.- Continued.

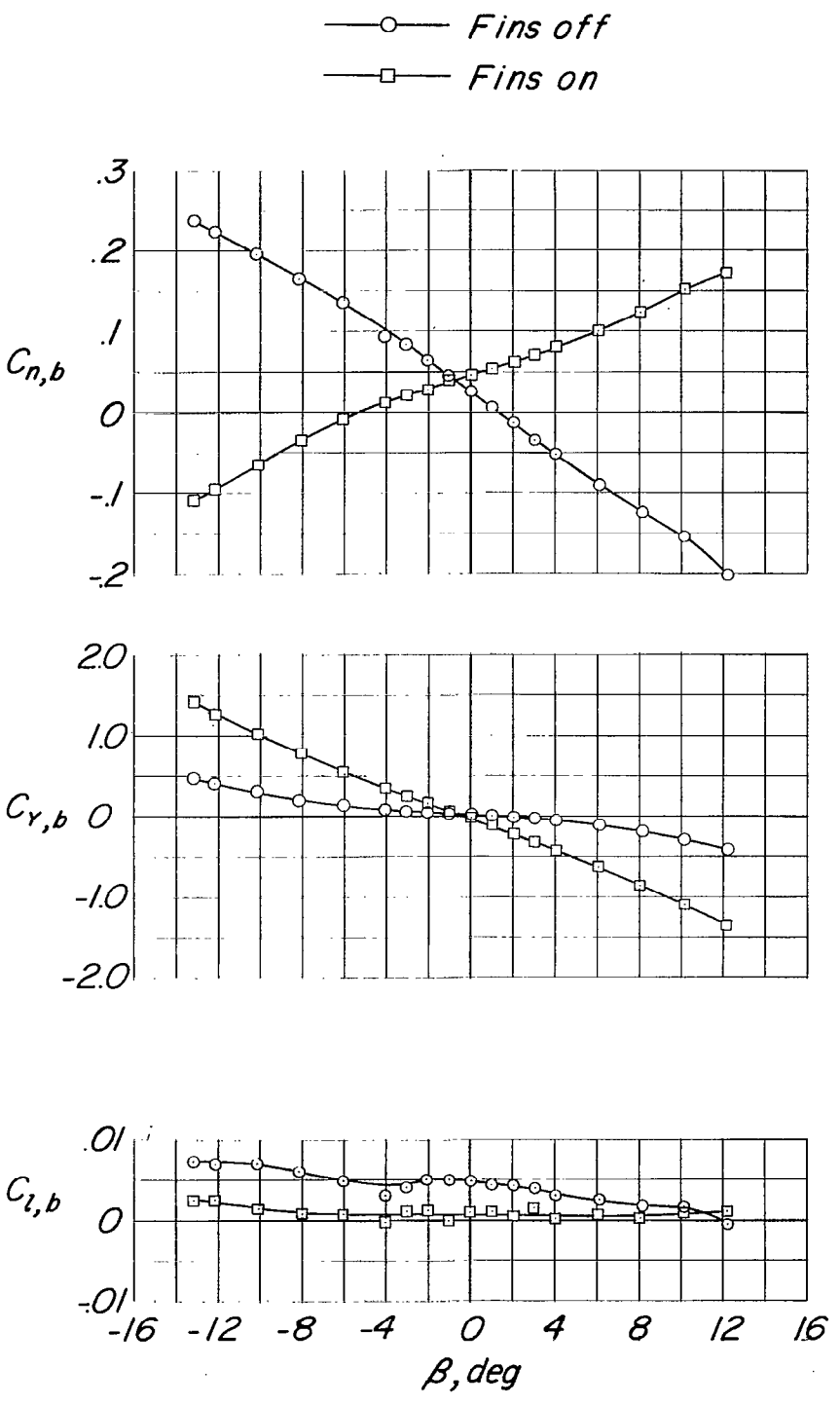

(b) Concluded.

Figure 6.- Continued.

[redacted]

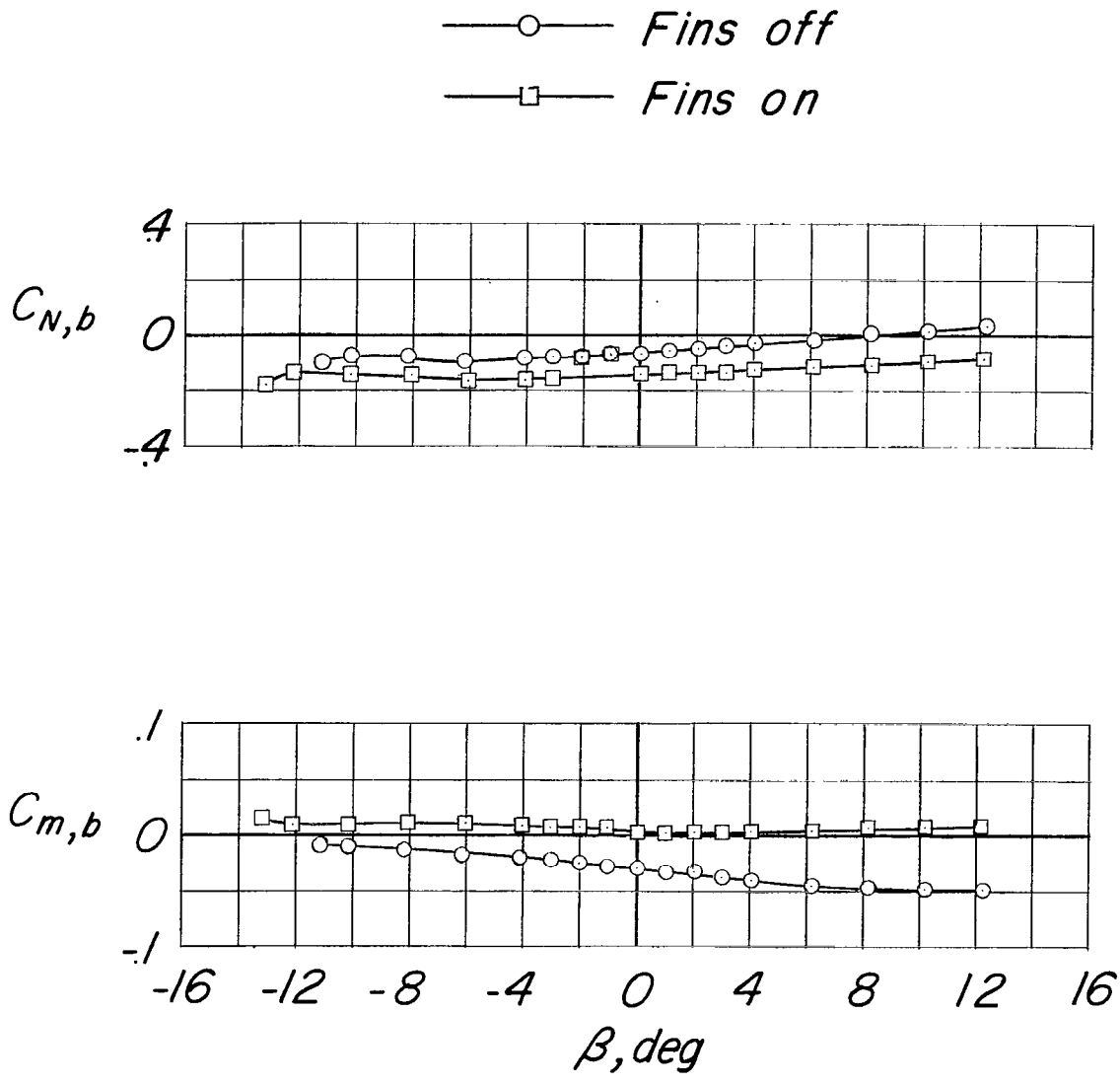

(c) M = 0.80; $\alpha = 0^{\circ}$; $C_L = -0.012$.

Figure 6.- Continued.

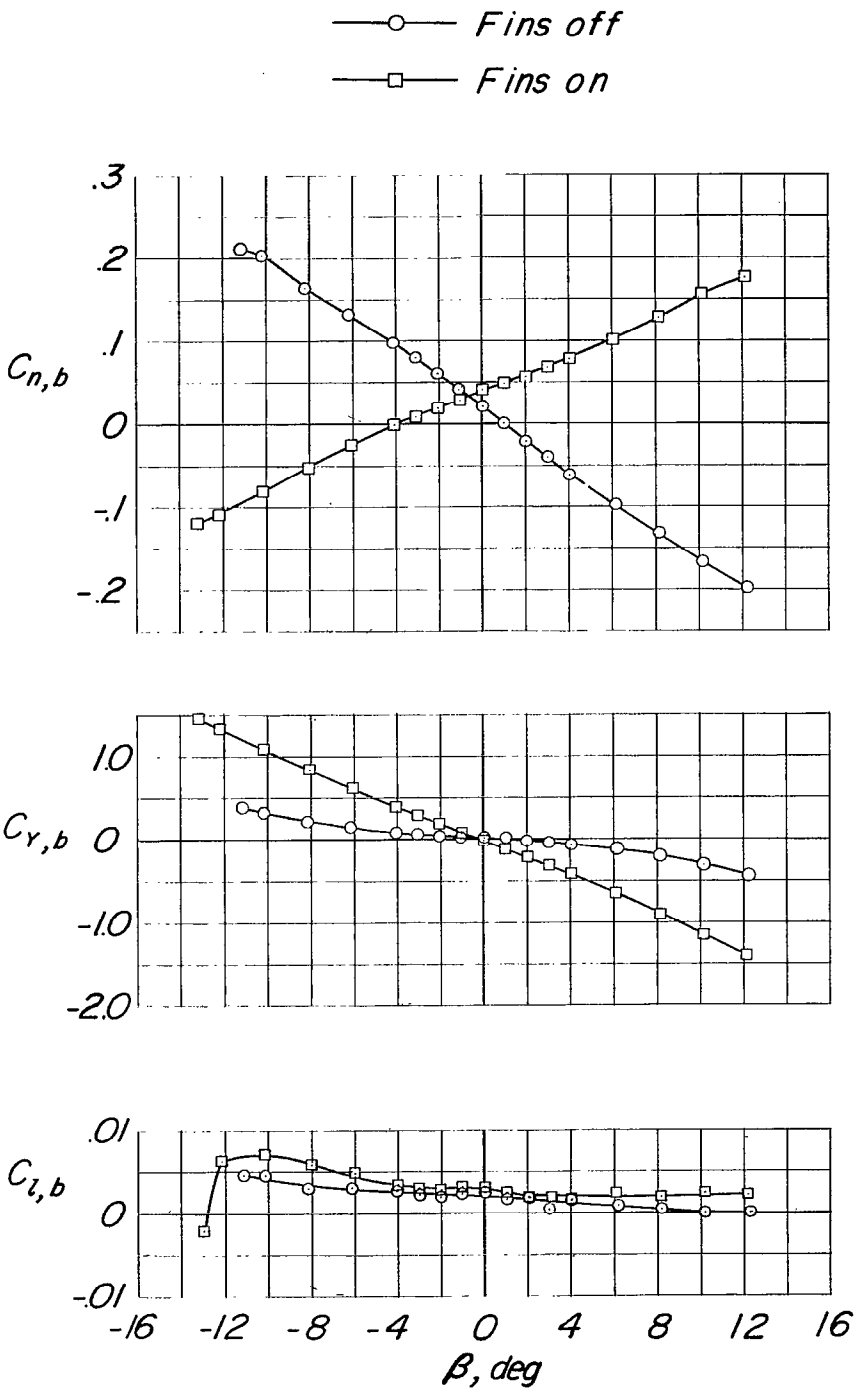

(c) Concluded.

Figure 6.- Continued.

[redacted]

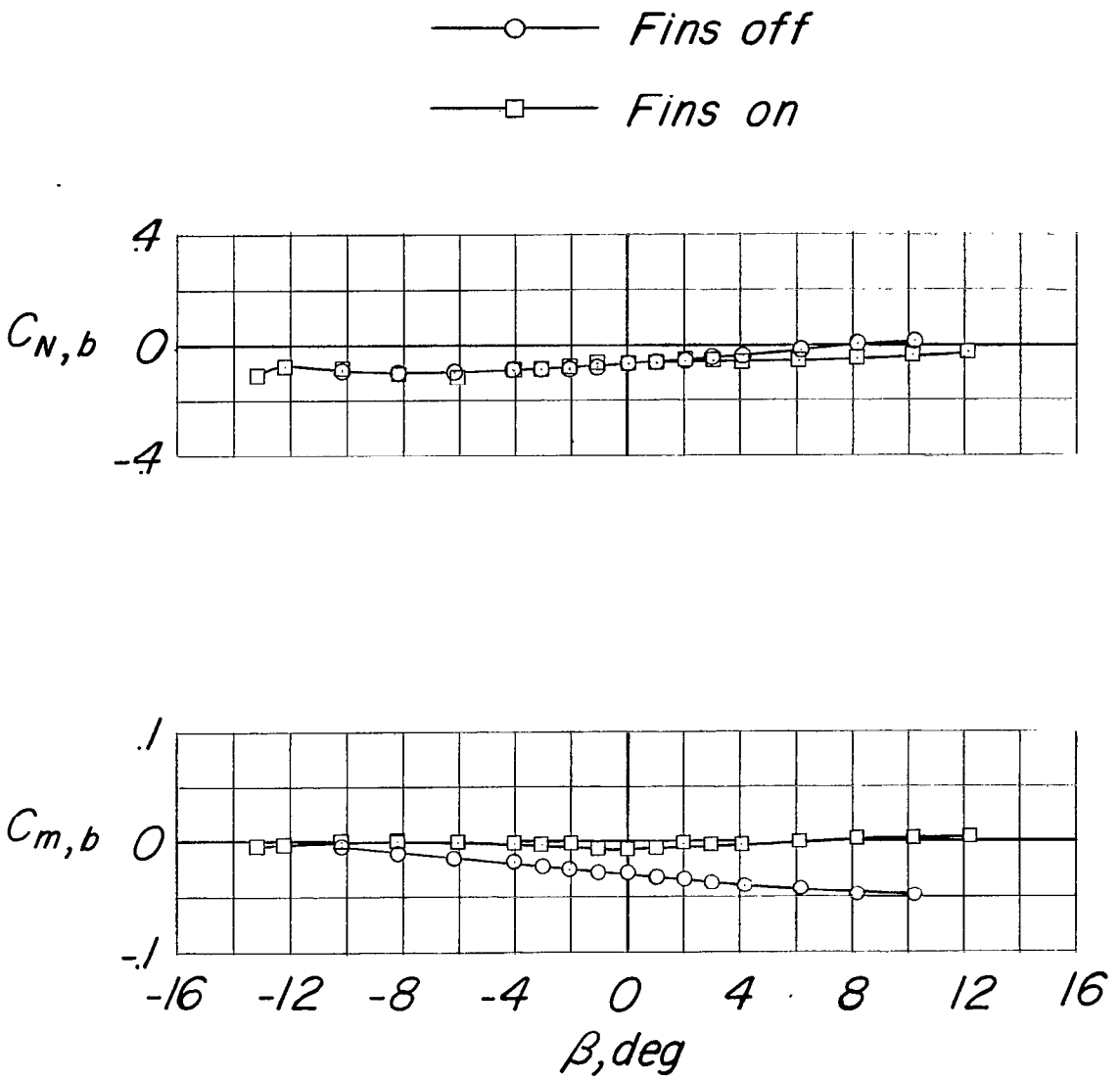

(d) M = 0.86; $\alpha = 0^{\circ}$; $C_L = -0.012$.

Figure 6.- Continued.

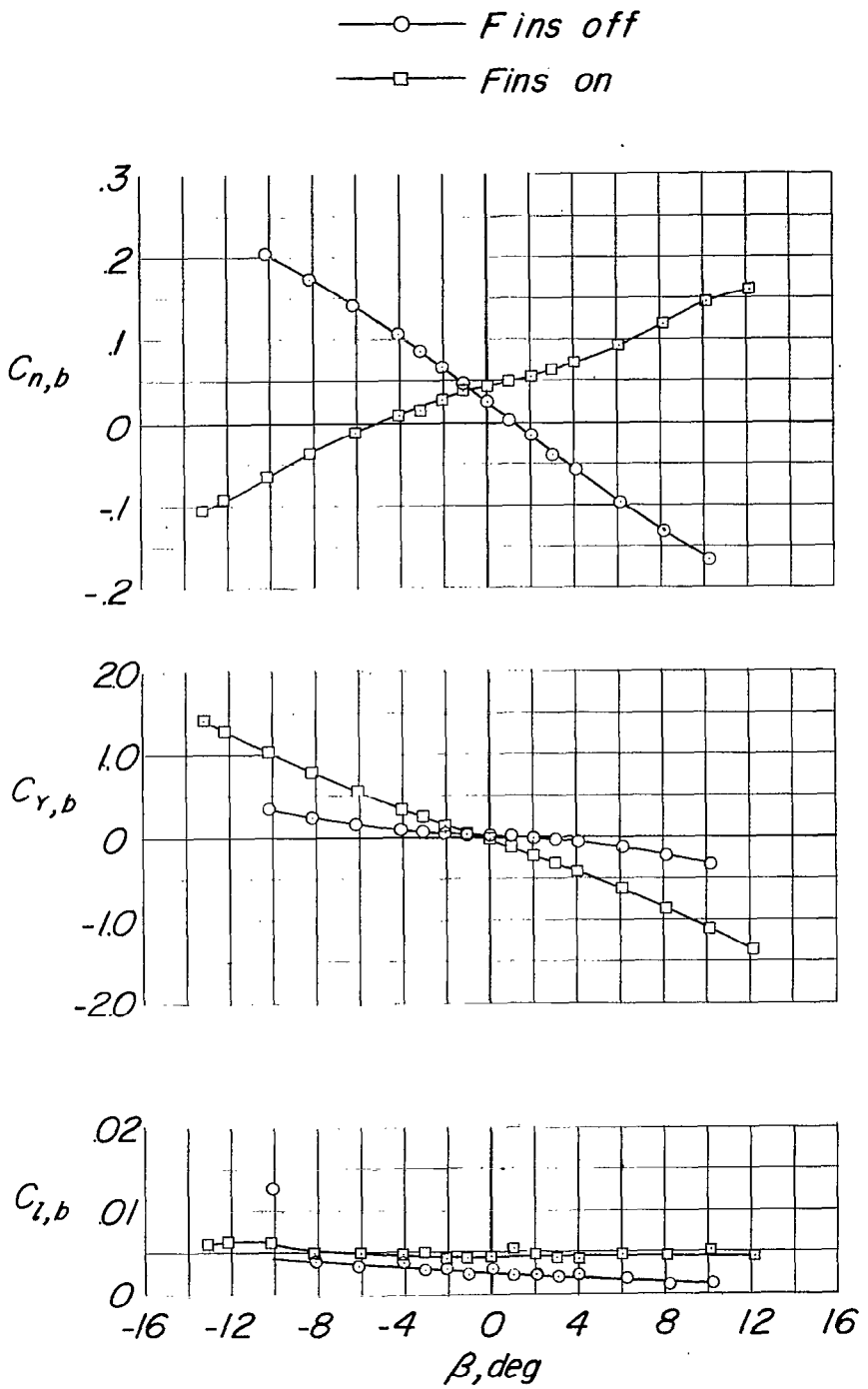

(d) Concluded.

Figure 6.- Continued.

[redacted]

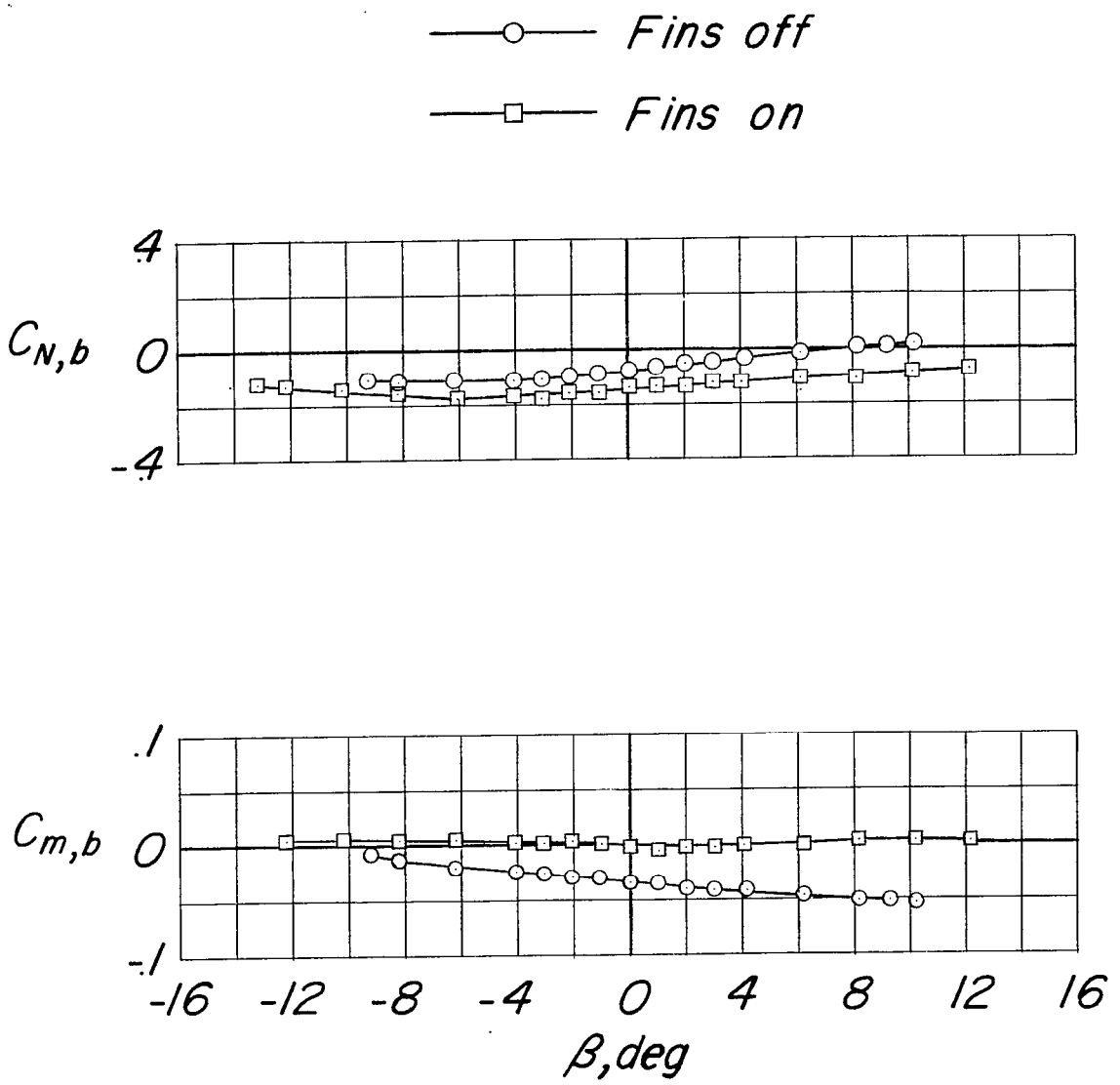

(e) M = 0.91; $\alpha = 0^\circ$; $C_L = -0.014$.

Figure 6.- Continued.

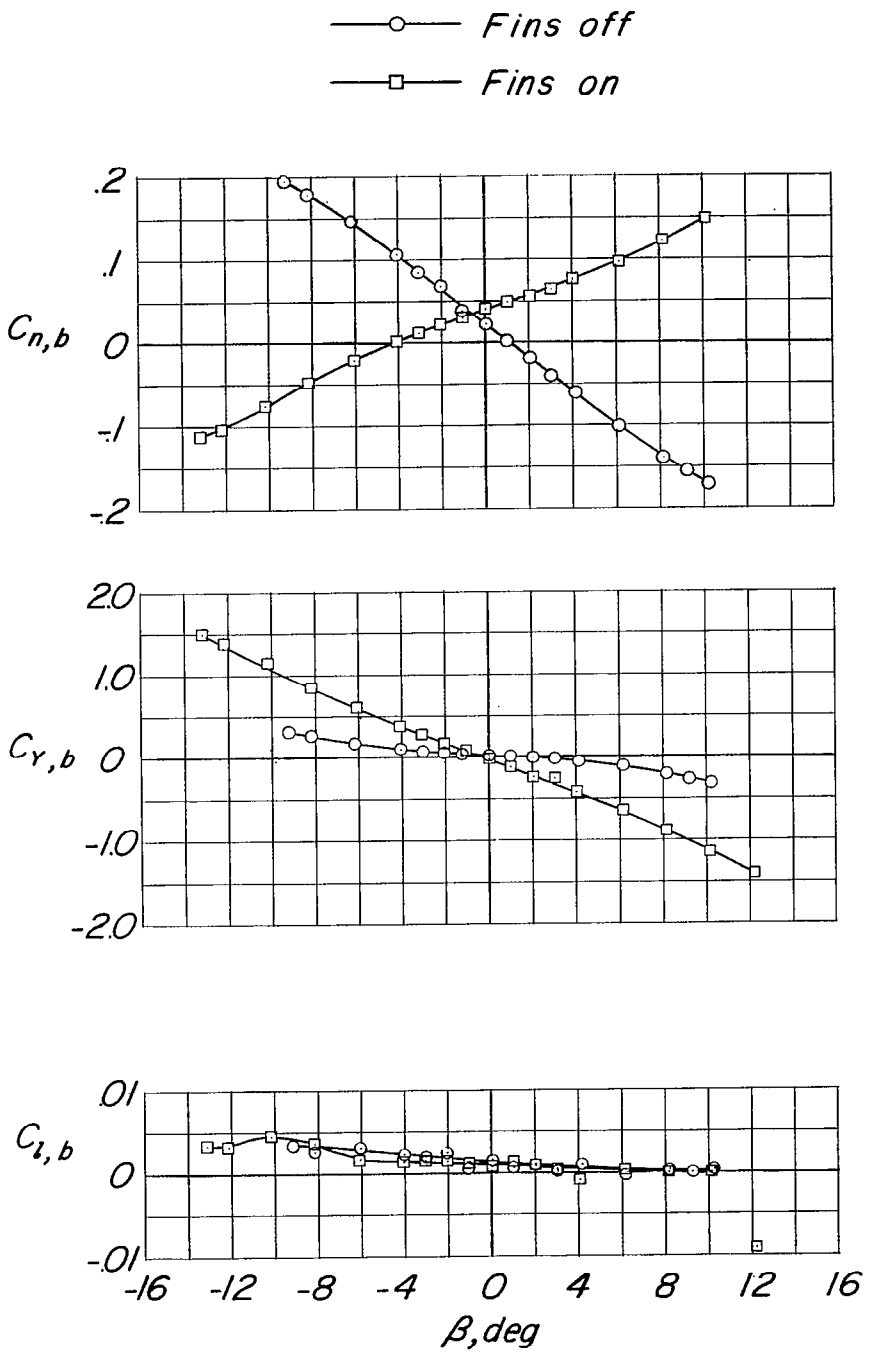

(e) Concluded.

Figure 6.- Continued.

[redacted]

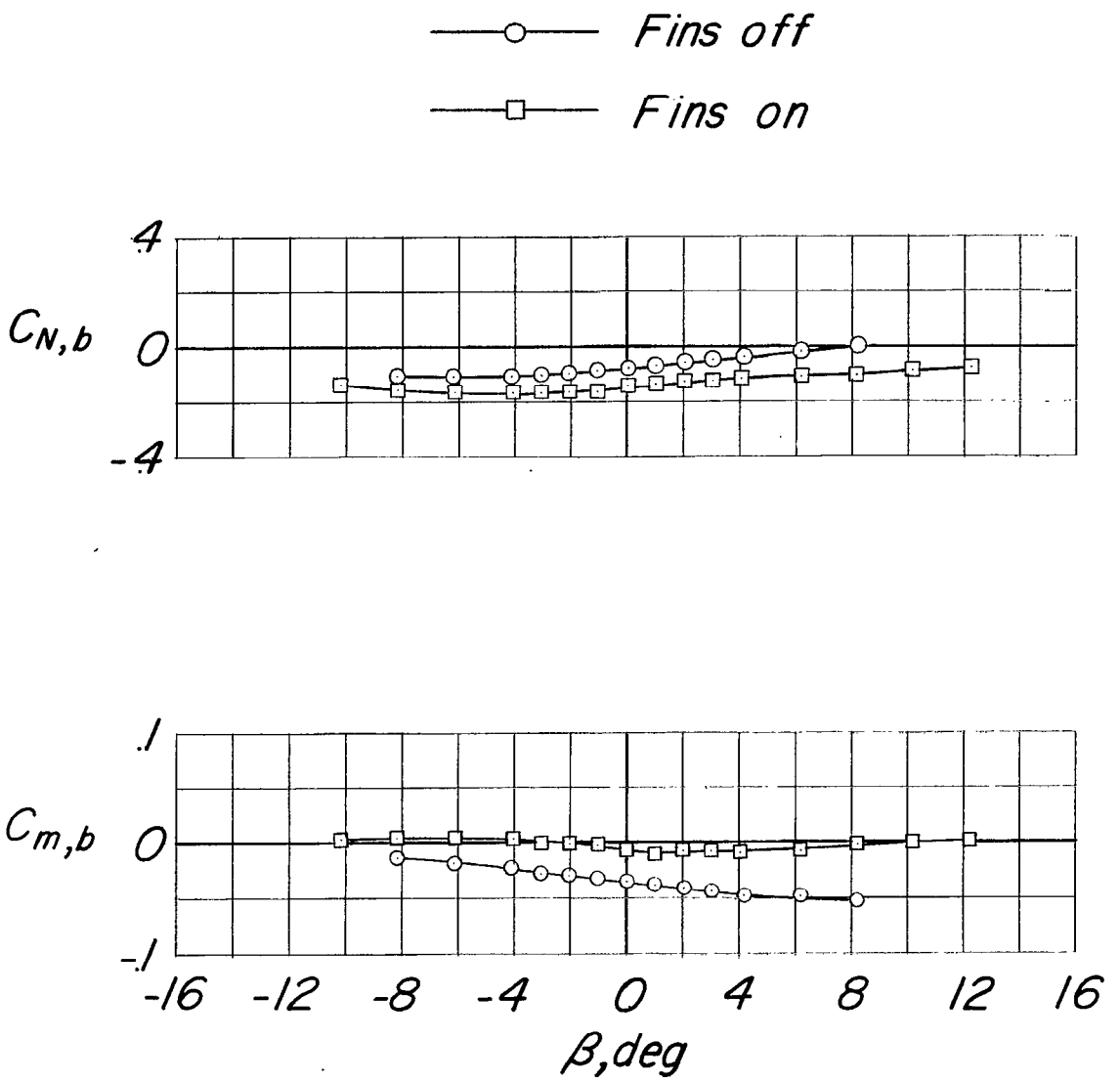

(f) M = 0.94; $\alpha = 0^{\circ}$; $C_L = -0.013$.

Figure 6.- Continued.

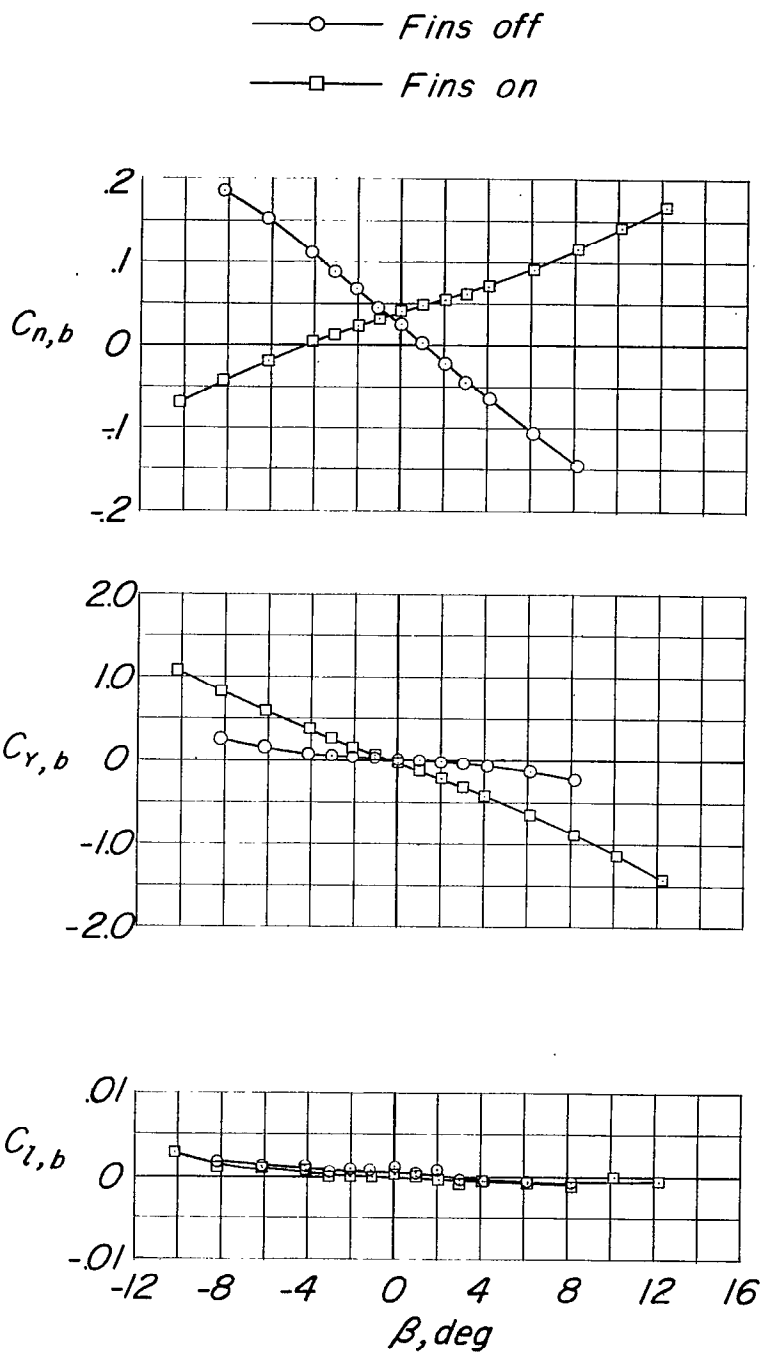

(f) Concluded.

Figure 6.- Concluded.

[redacted]

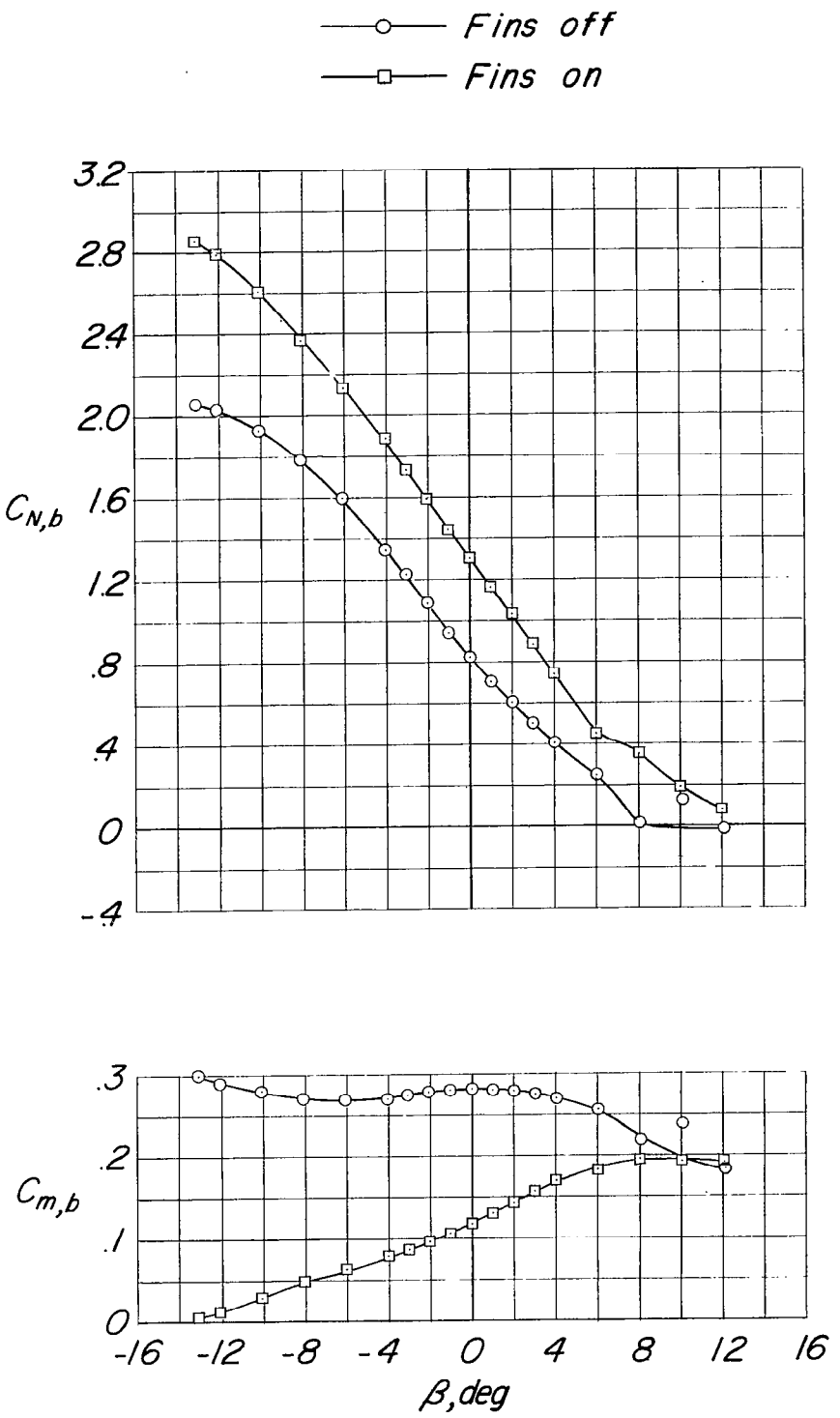

(a) M = 0.50; $\alpha = 6.3^{\circ}$; $C_L = 0.392$.

Figure 7.- Aerodynamic characteristics of the body mounted on the left wing tip of the swept-wing—fuselage model.

[redacted]

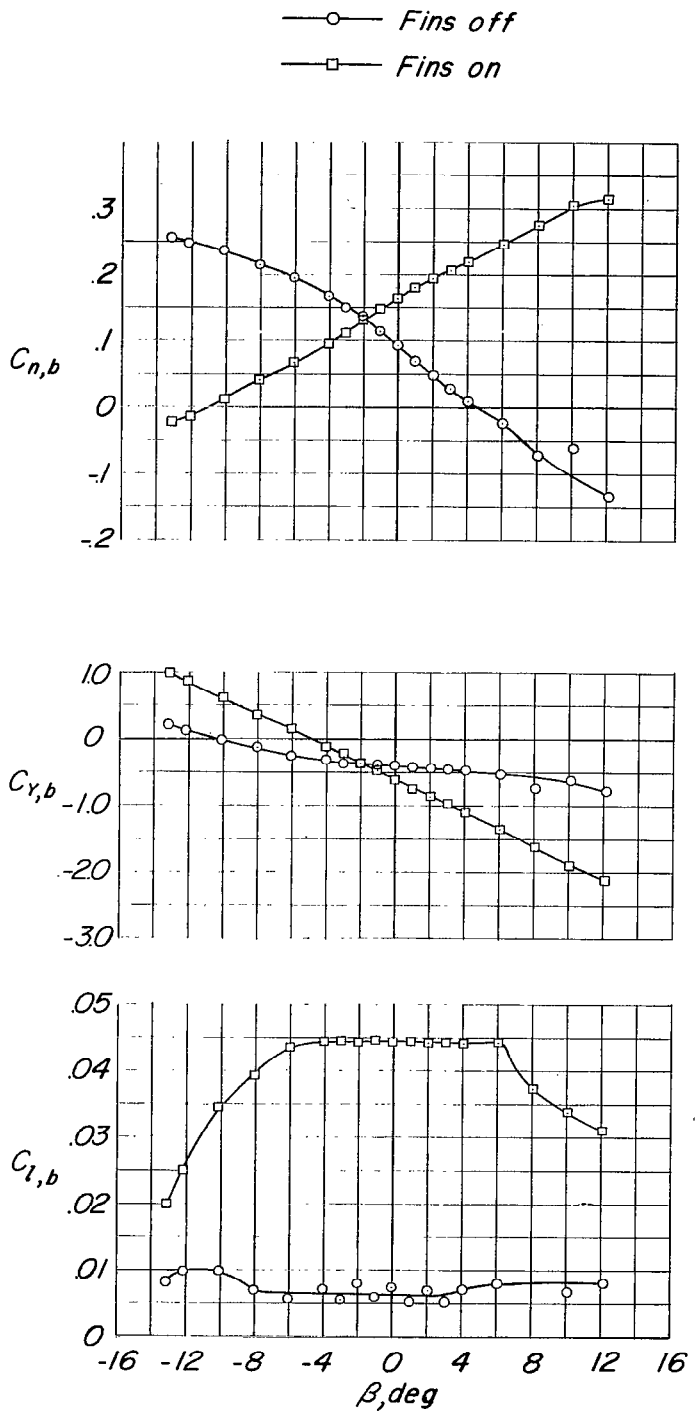

(a) Concluded.

Figure 7.- Continued.

[redacted]

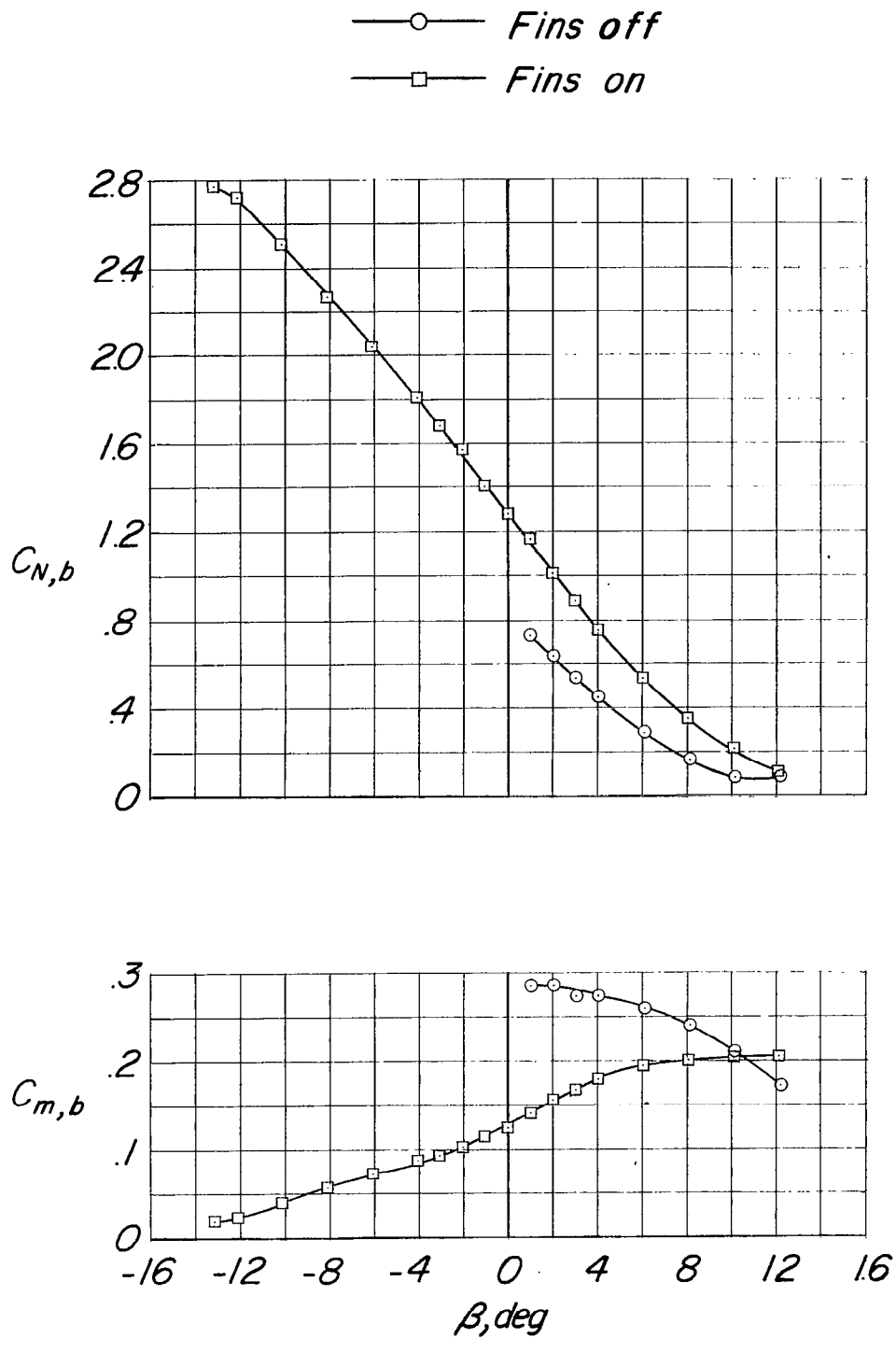

(b) M = 0.70; $\alpha = 6.5^{\circ}$; $C_L = 0.410$.

Figure 7.- Continued.

[redacted]

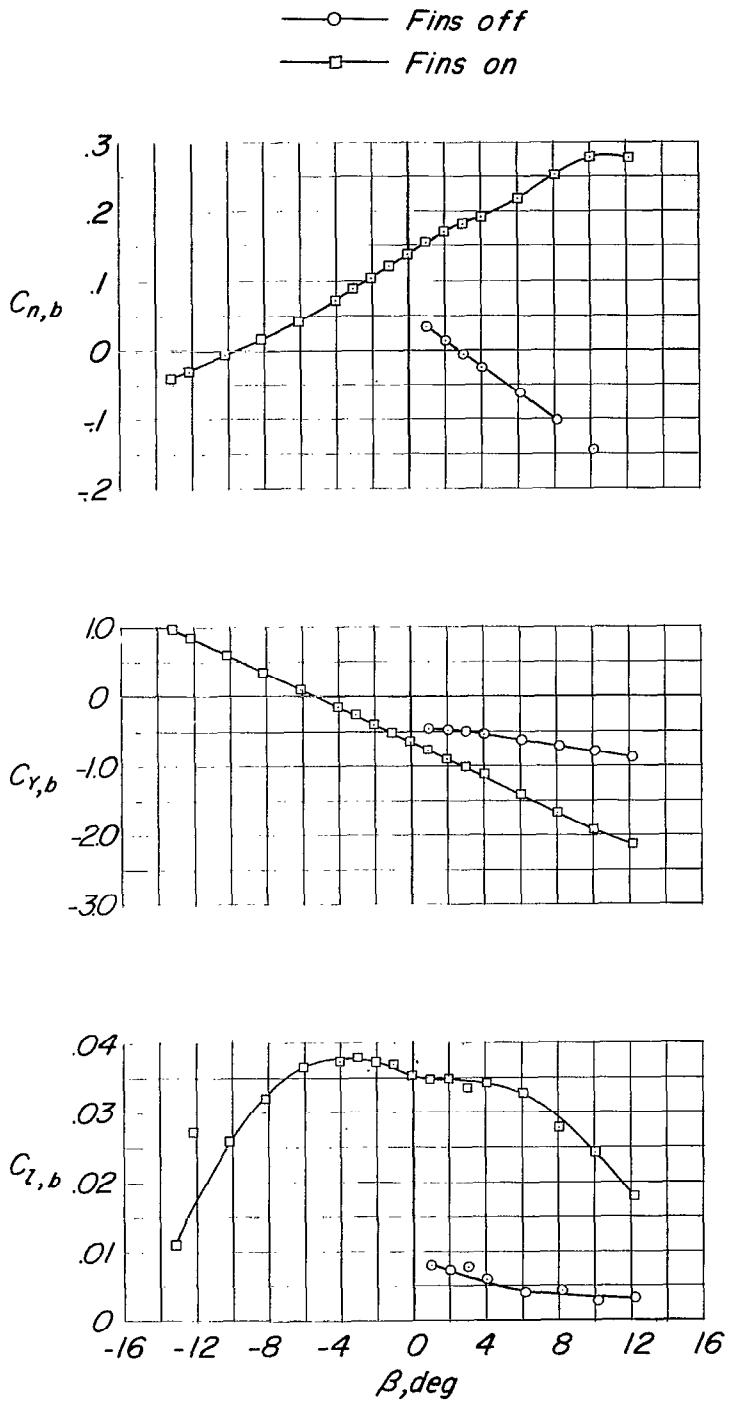

(b) Concluded.

Figure 7.- Continued.

[redacted]

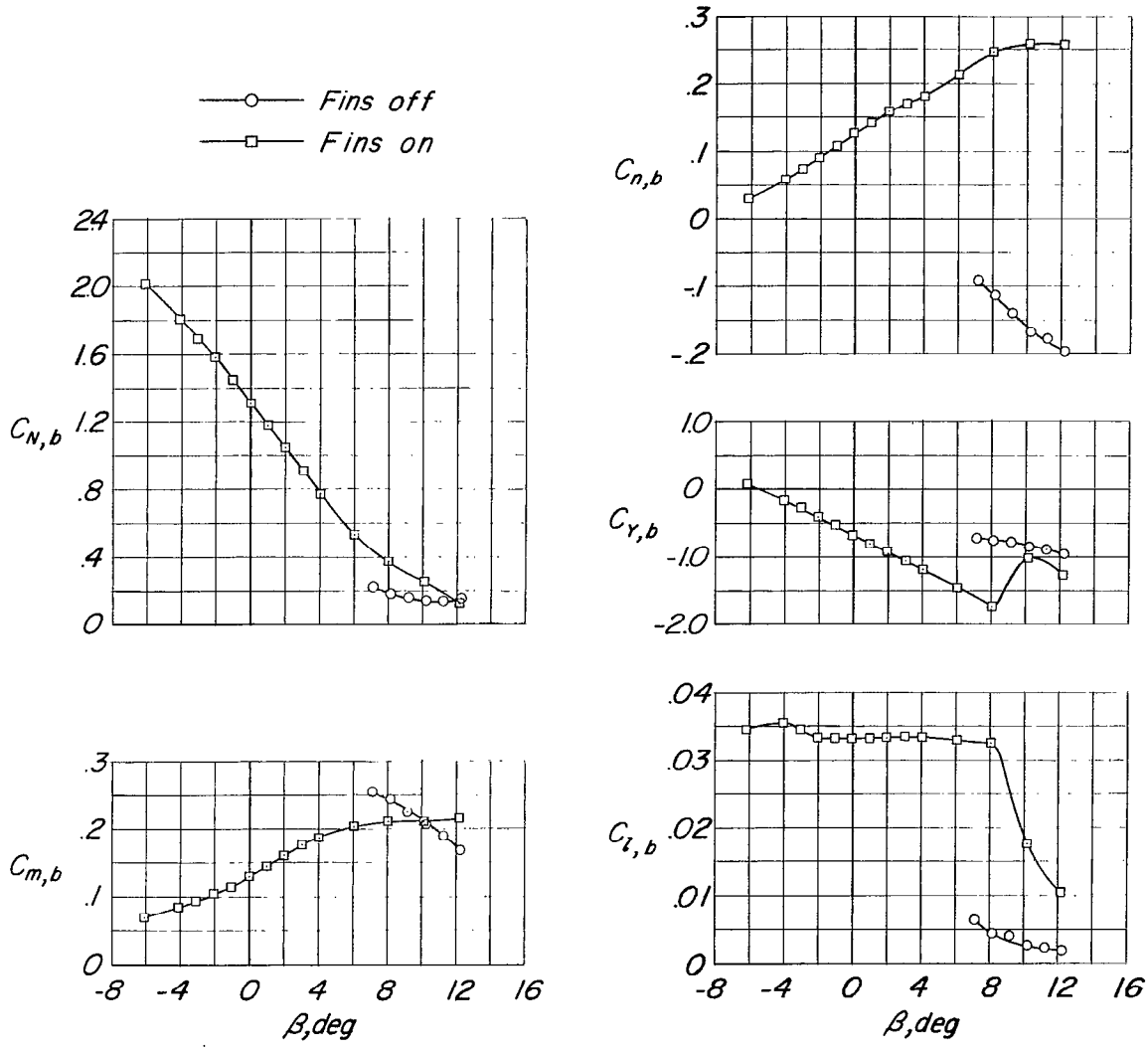

(c) M = 0.80; $\alpha = 6.5^{\circ}$; $C_L = 0.428$.

Figure 7.- Continued.

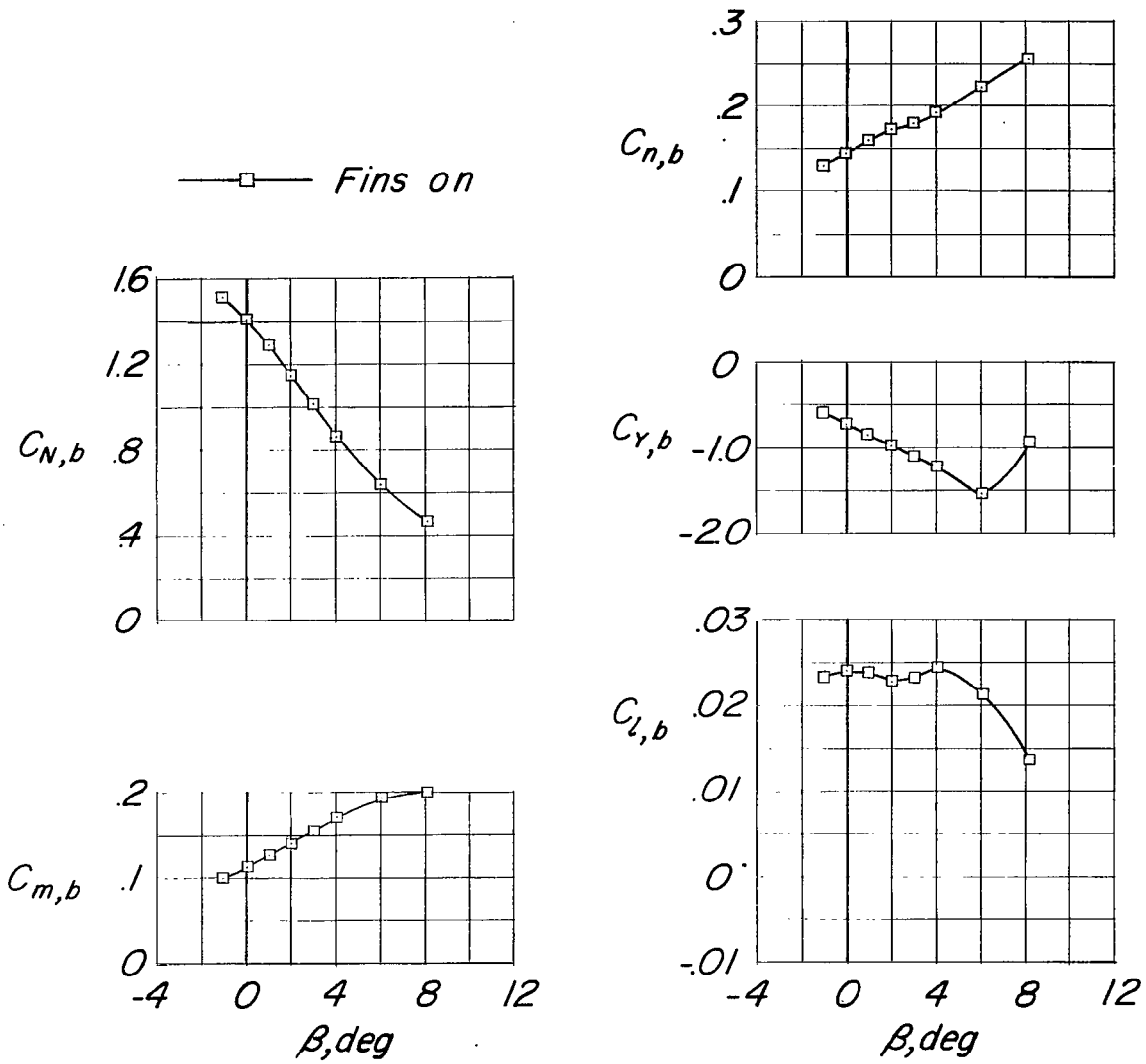

(d) M = 0.86; α = 6.6°; C_L = 0.456.

Figure 7.- Concluded.

[redacted]

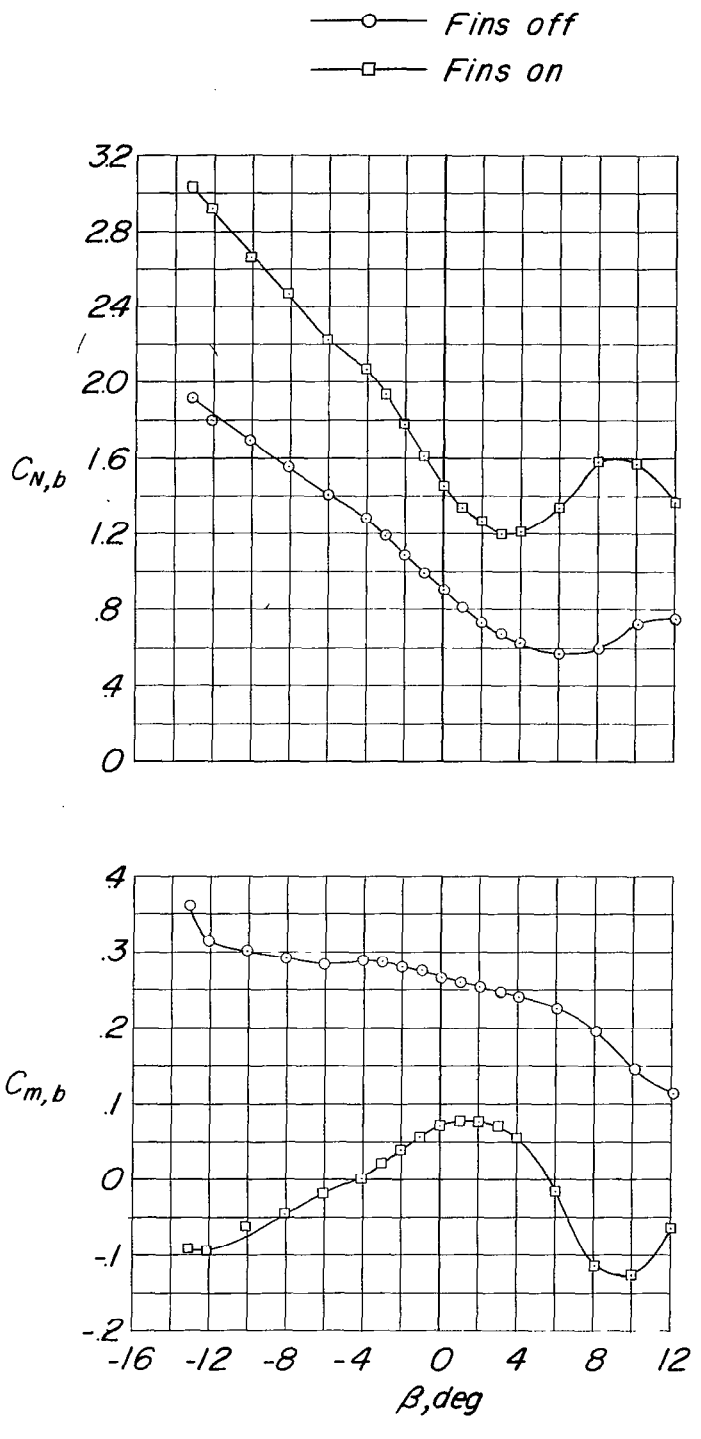

(a) M = 0.50; α = 12.6°; C_L = 0.796.

Figure 8.- Aerodynamic characteristics of the body mounted on the left wing tip of the swept-wing—fuselage model.

[redacted]

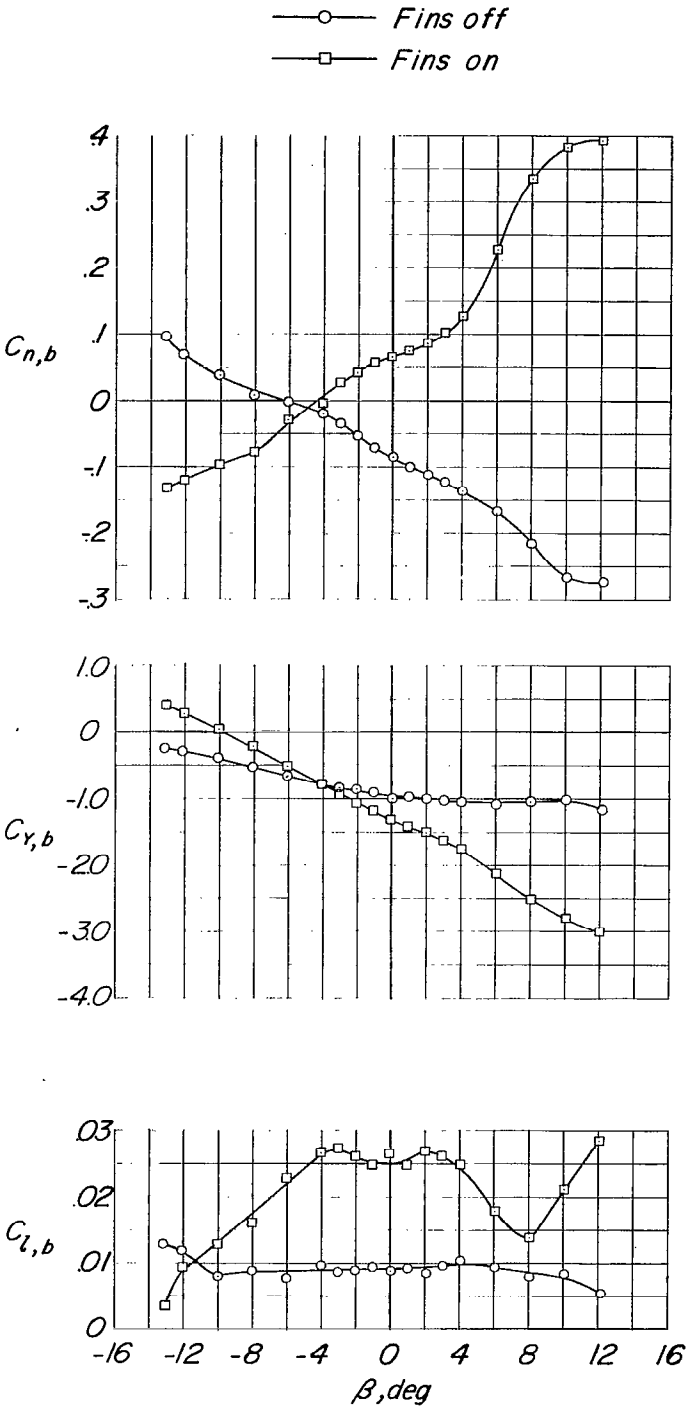

(a) Concluded.

Figure 8.- Continued.

[redacted]

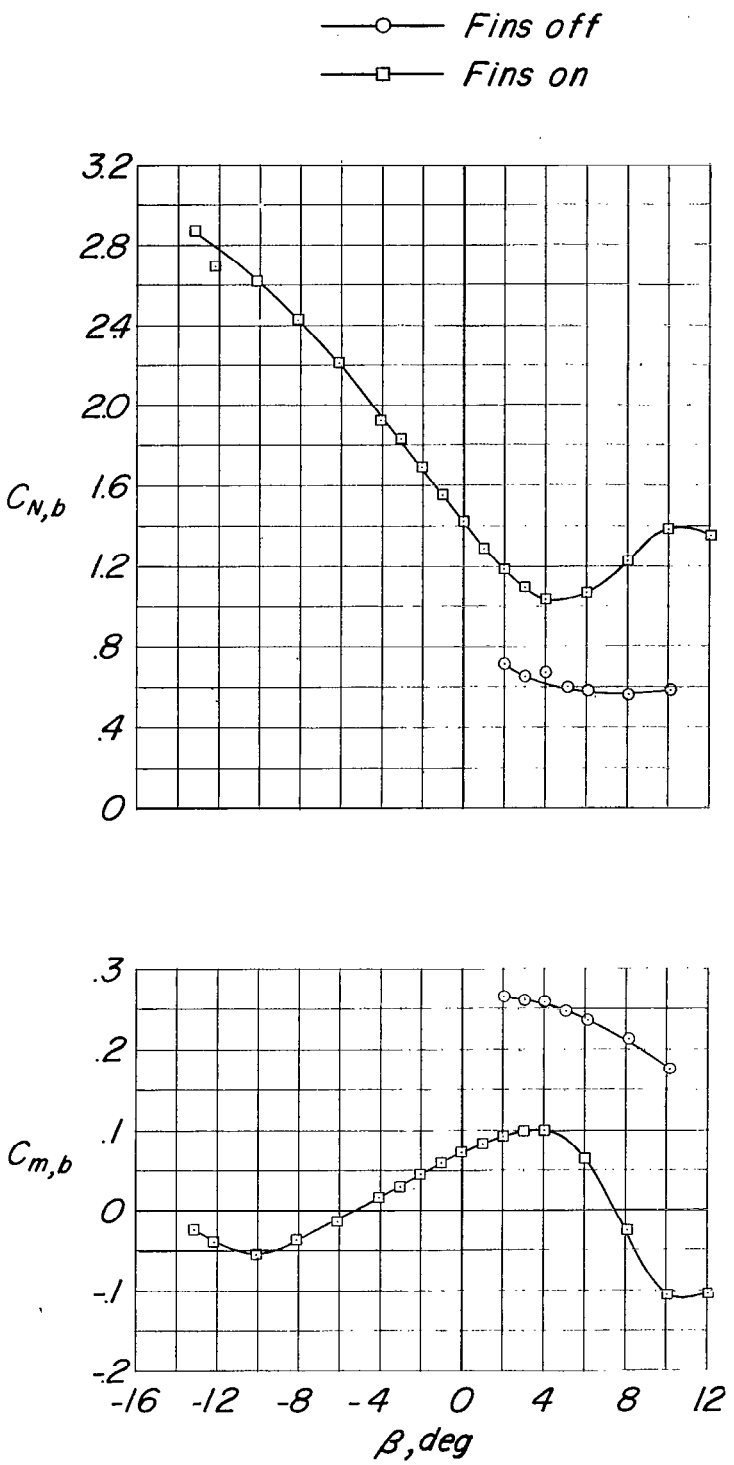

(b) M = 0.70; $\alpha = 12.9^{\circ}$; $C_L = 0.778$.

Figure 8.- Continued.

[redacted]

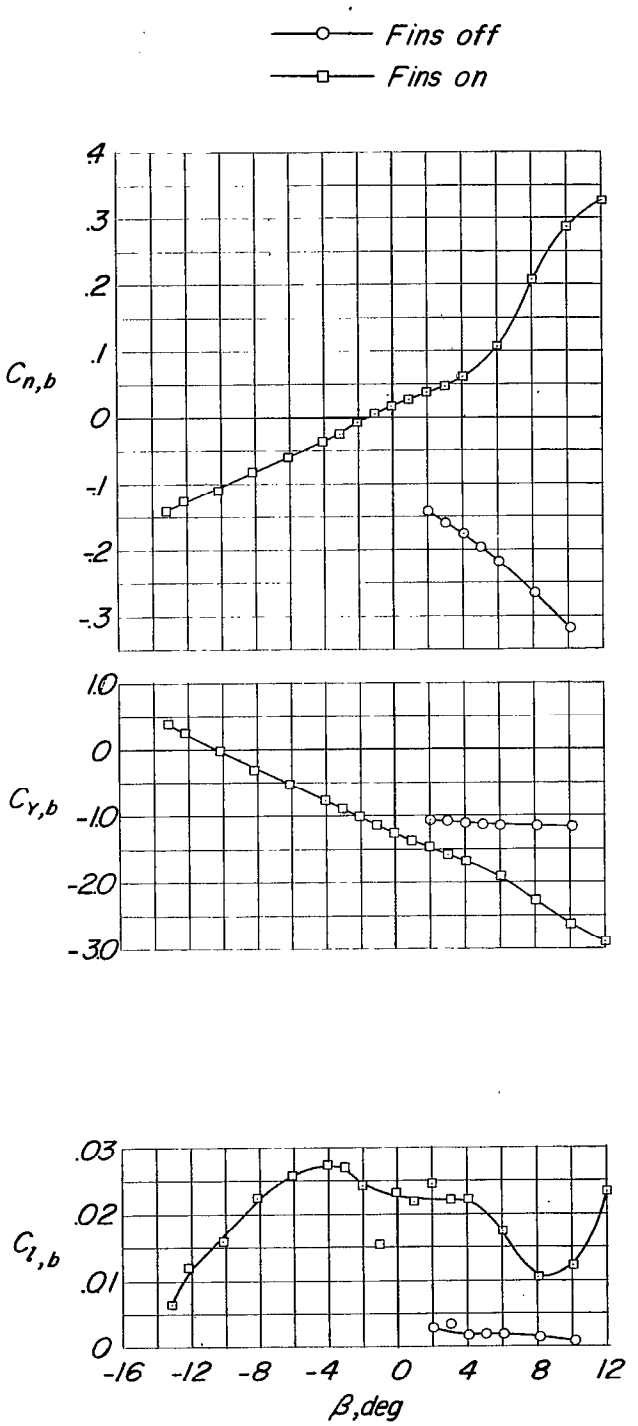

(b) Concluded.

Figure 8.- Continued.

[redacted]

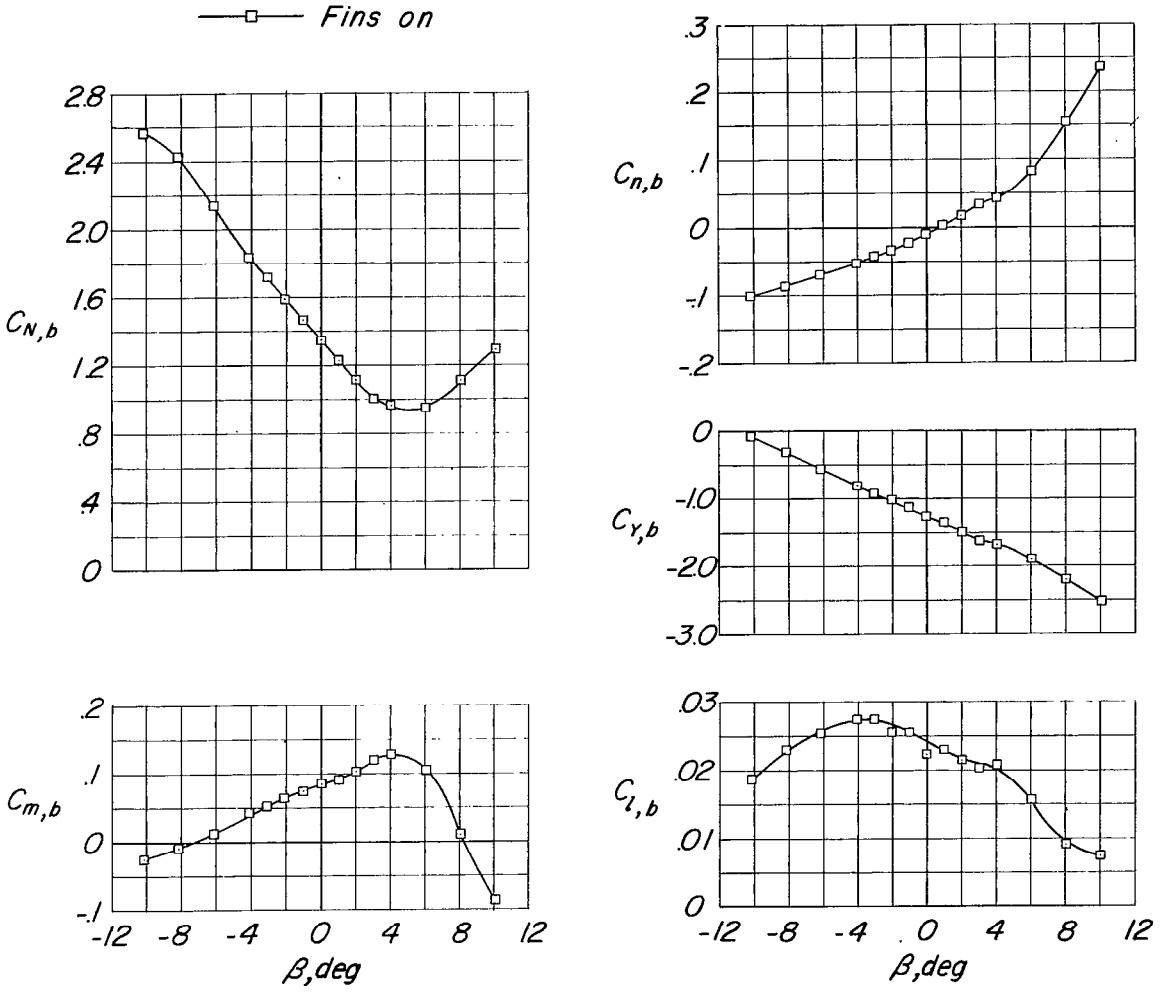

(c) M = 0.80; α = 13.1°; C_L = 0.779.

Figure 8.- Continued.

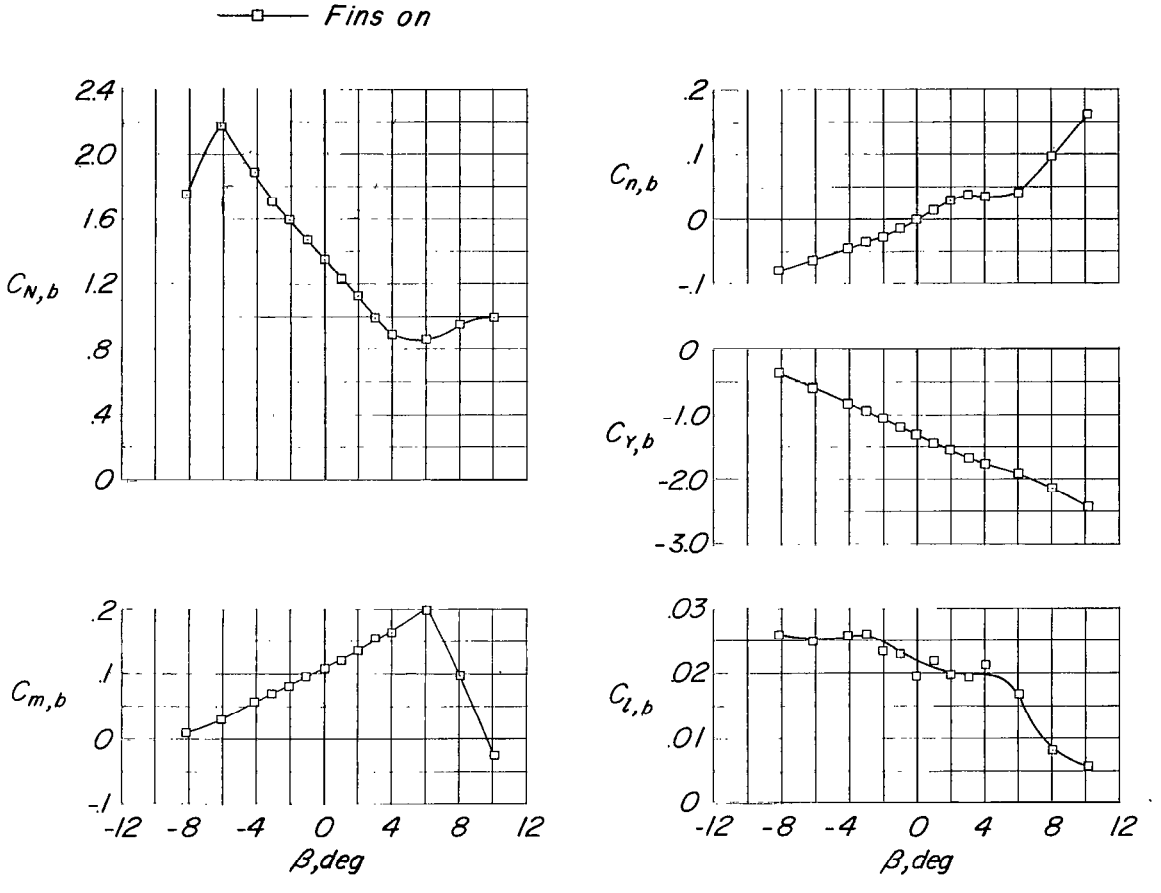

(d) M = 0.86; α = 13.1°; C_L = 0.764.

Figure 8.- Concluded.

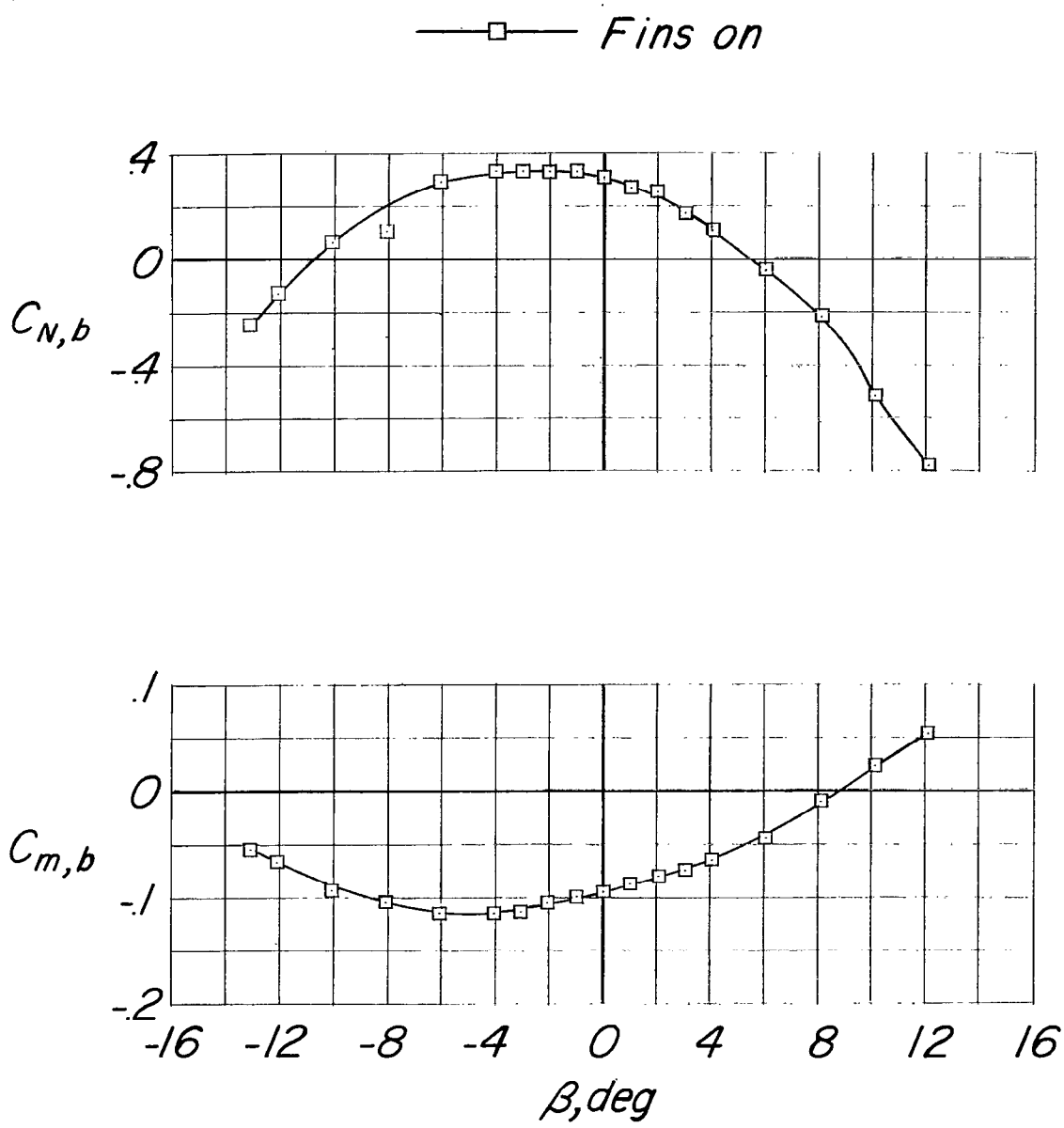

(a) M = 0.50; $\alpha = 6.3^{\circ}$; $C_L = 0.356$.

Figure 9.- Aerodynamic characteristics of the body mounted on the pylon on the left wing of the swept-wing—fuselage model.

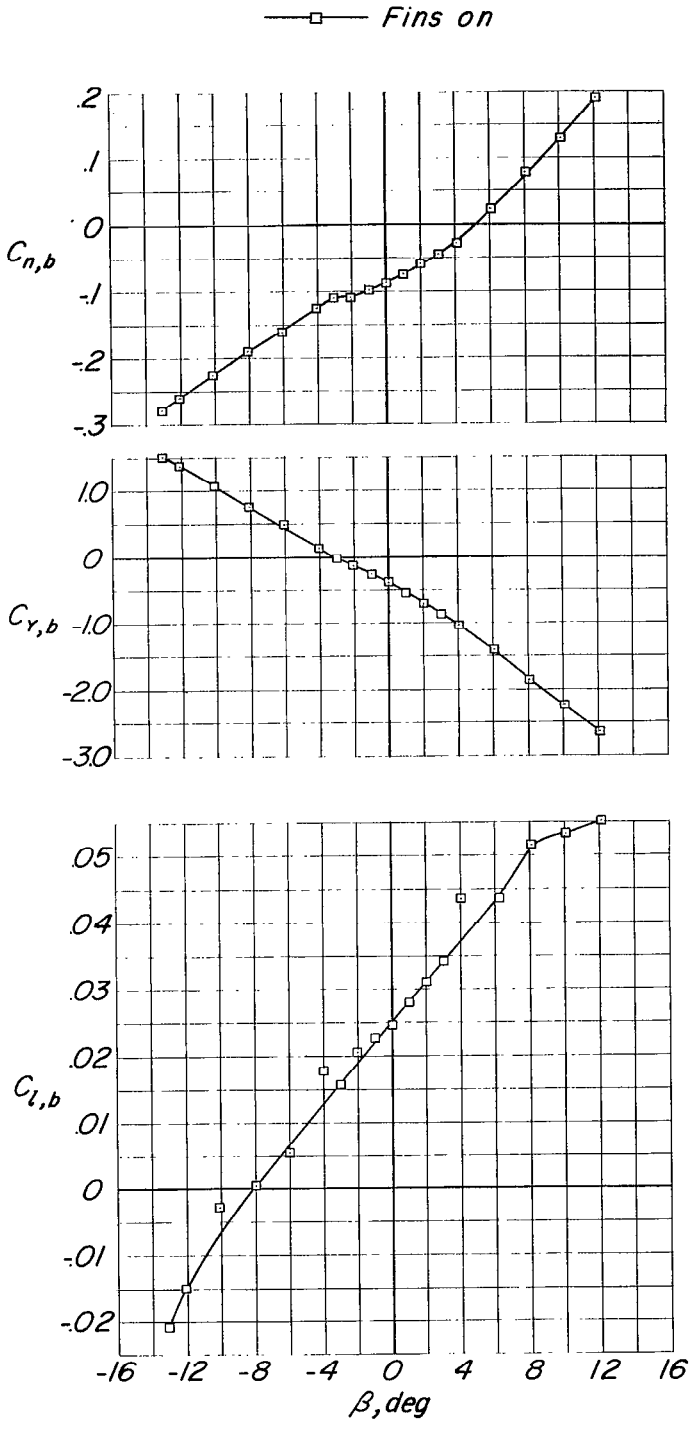

(a) Concluded.

Figure 9.- Continued.

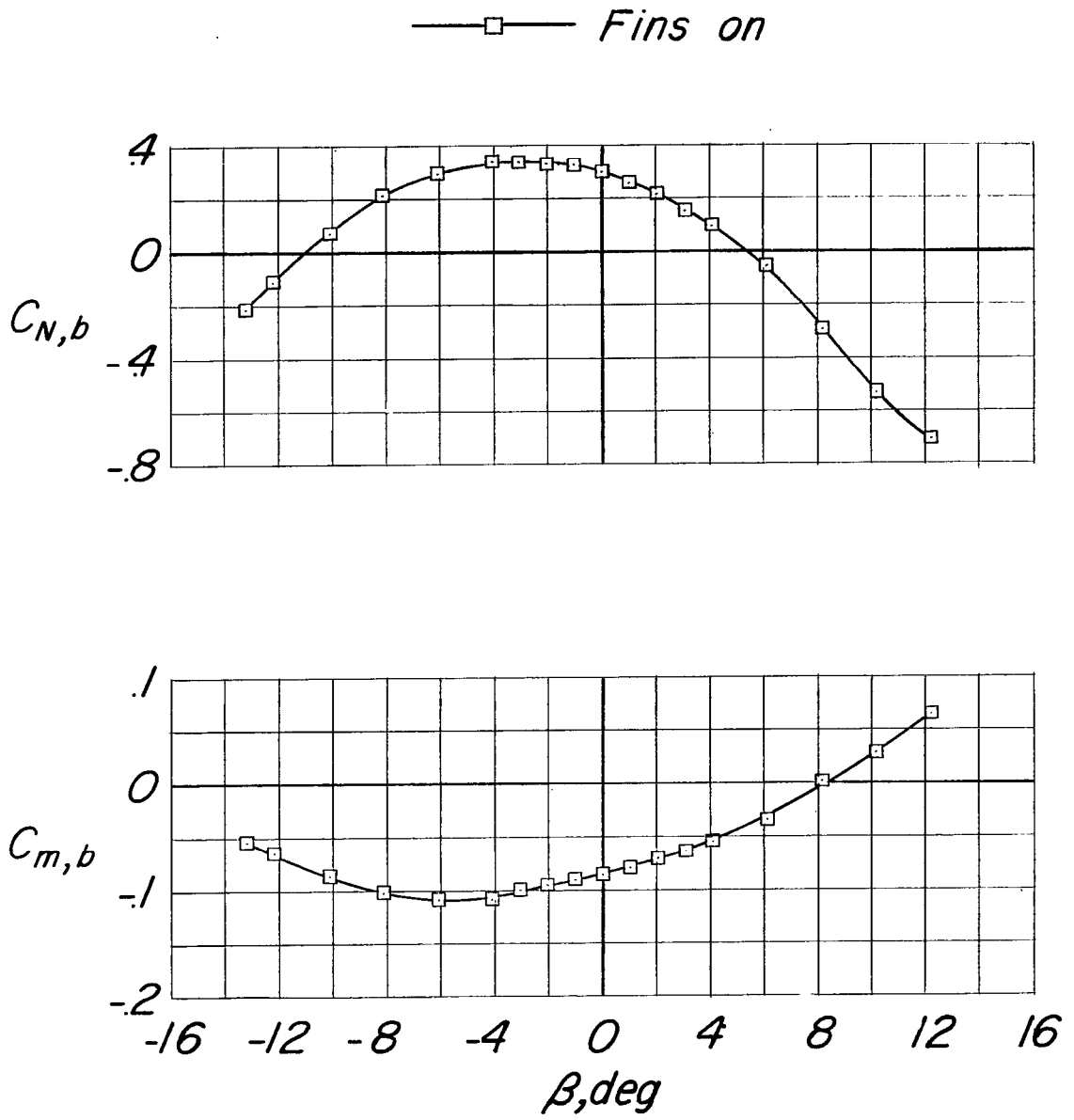

(b) M = 0.70; $\alpha = 6.5^{\circ}$; $C_L = 0.388$.

Figure 9.- Continued.

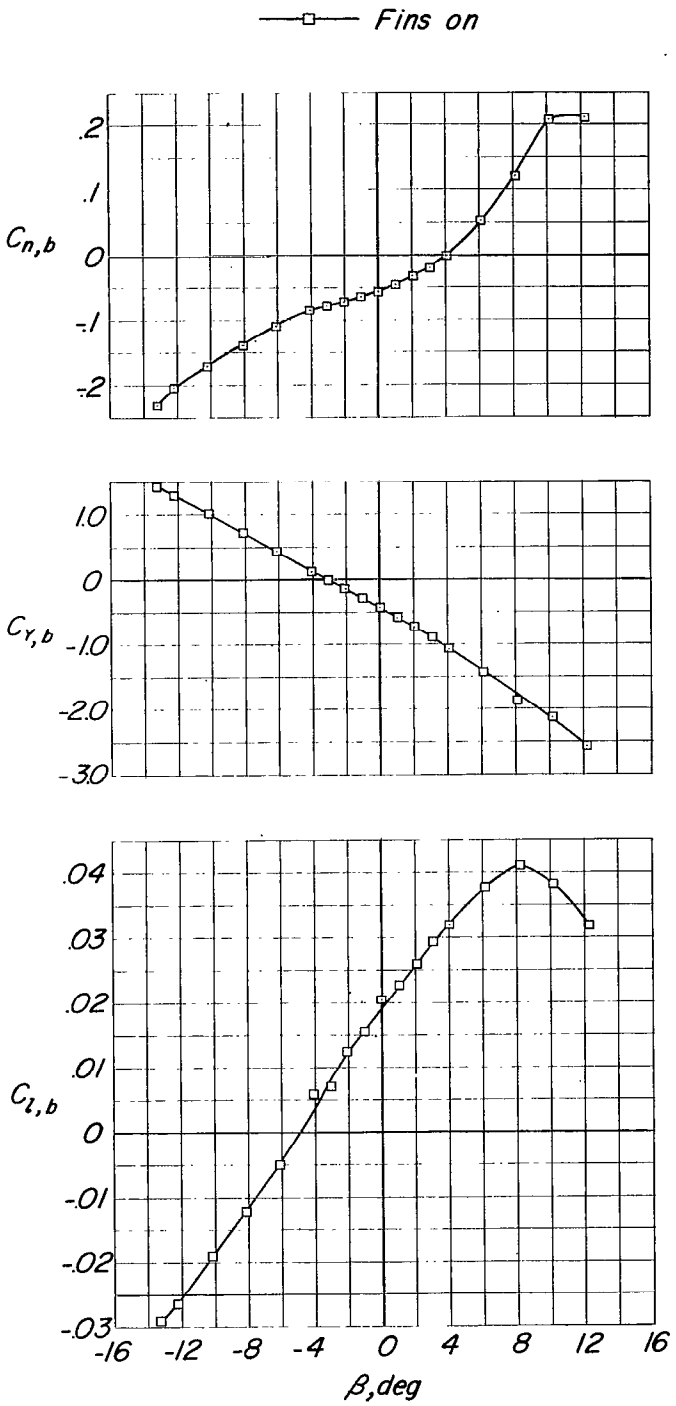

(b) Concluded.

Figure 9.- Concluded.

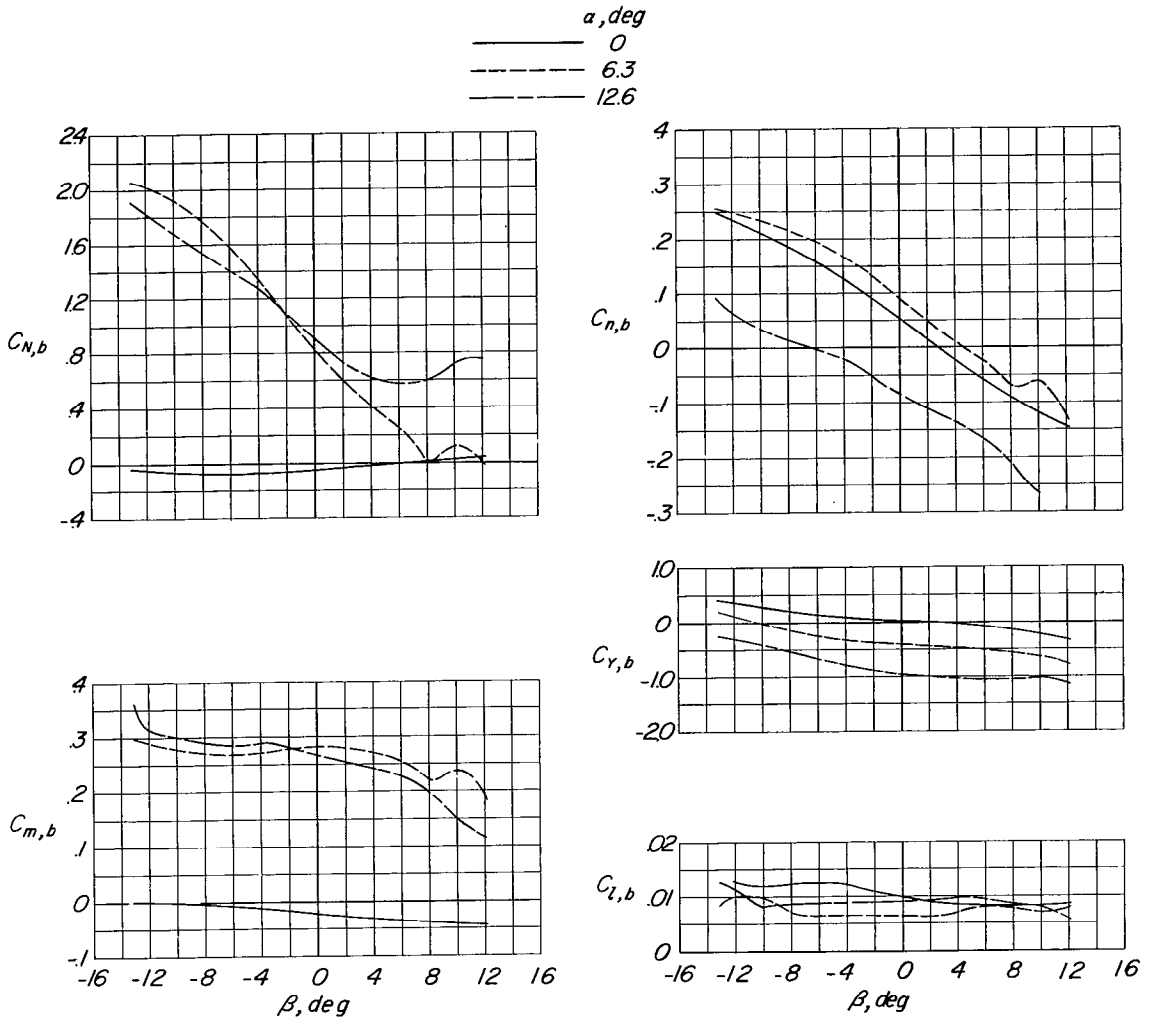

(a) Fins off.

Figure 10.- Comparison of aerodynamic characteristics of tip-mounted body at three angles of attack. M = 0.50.

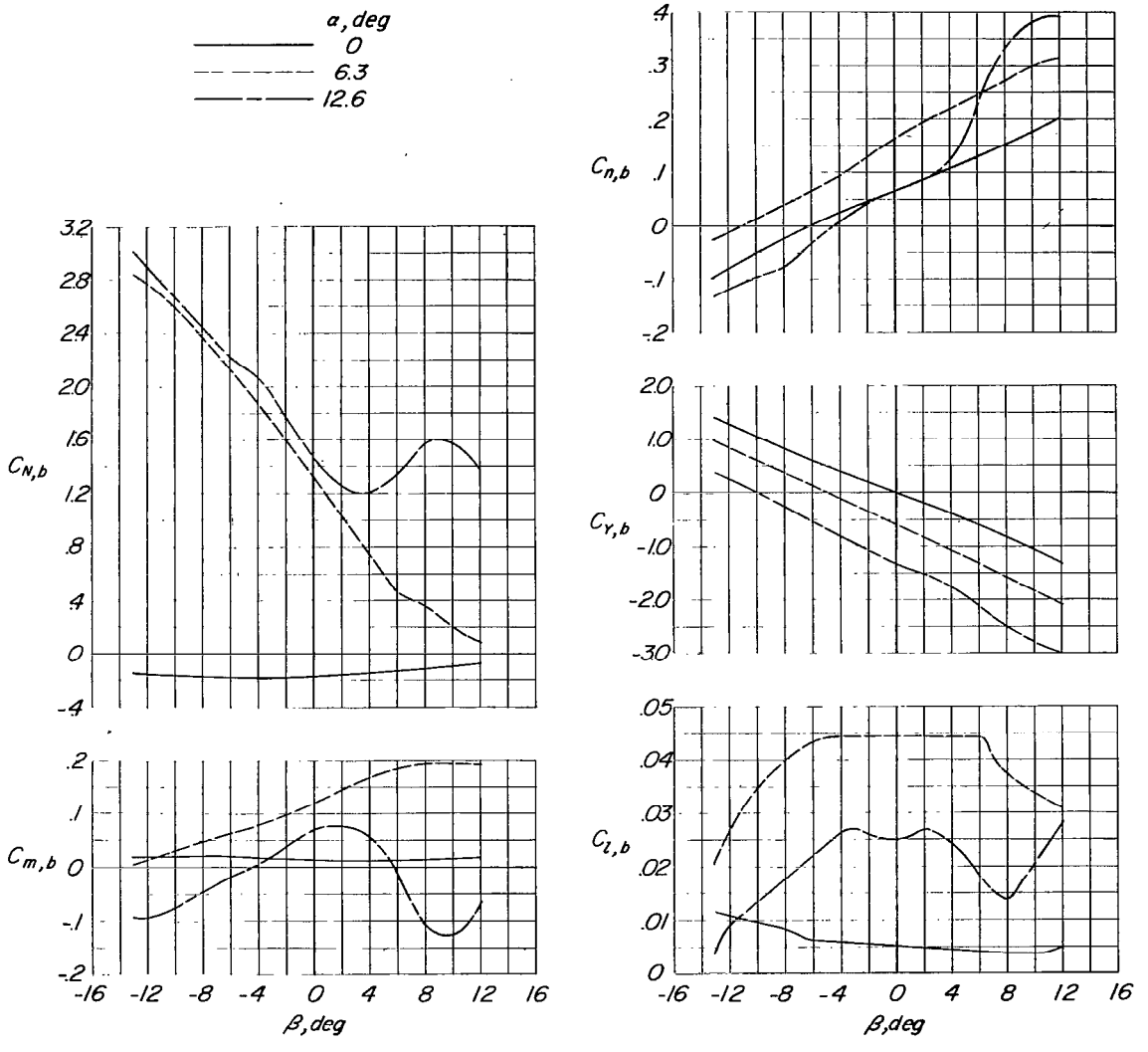

(b) Fins on.

Figure 10.- Concluded.

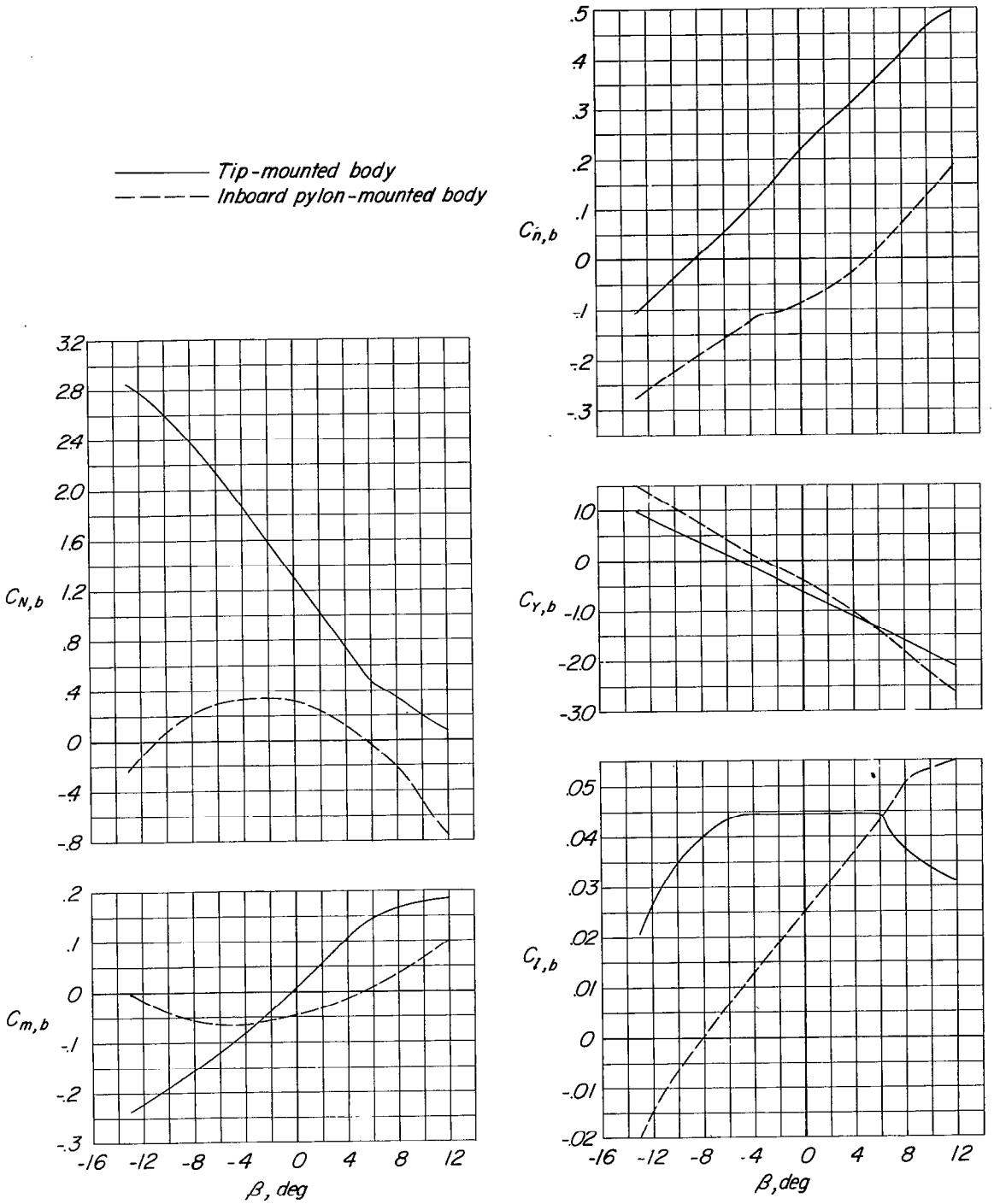

Figure 11.- Comparison of aerodynamic characteristics of a body mounted on the left wing tip and from a pylon under the left wing of a wing-fuselage model. Fins on; M = 0.50; $\alpha = 6.3^{\circ}$; moment center at $0.462l_b$.

[redacted]

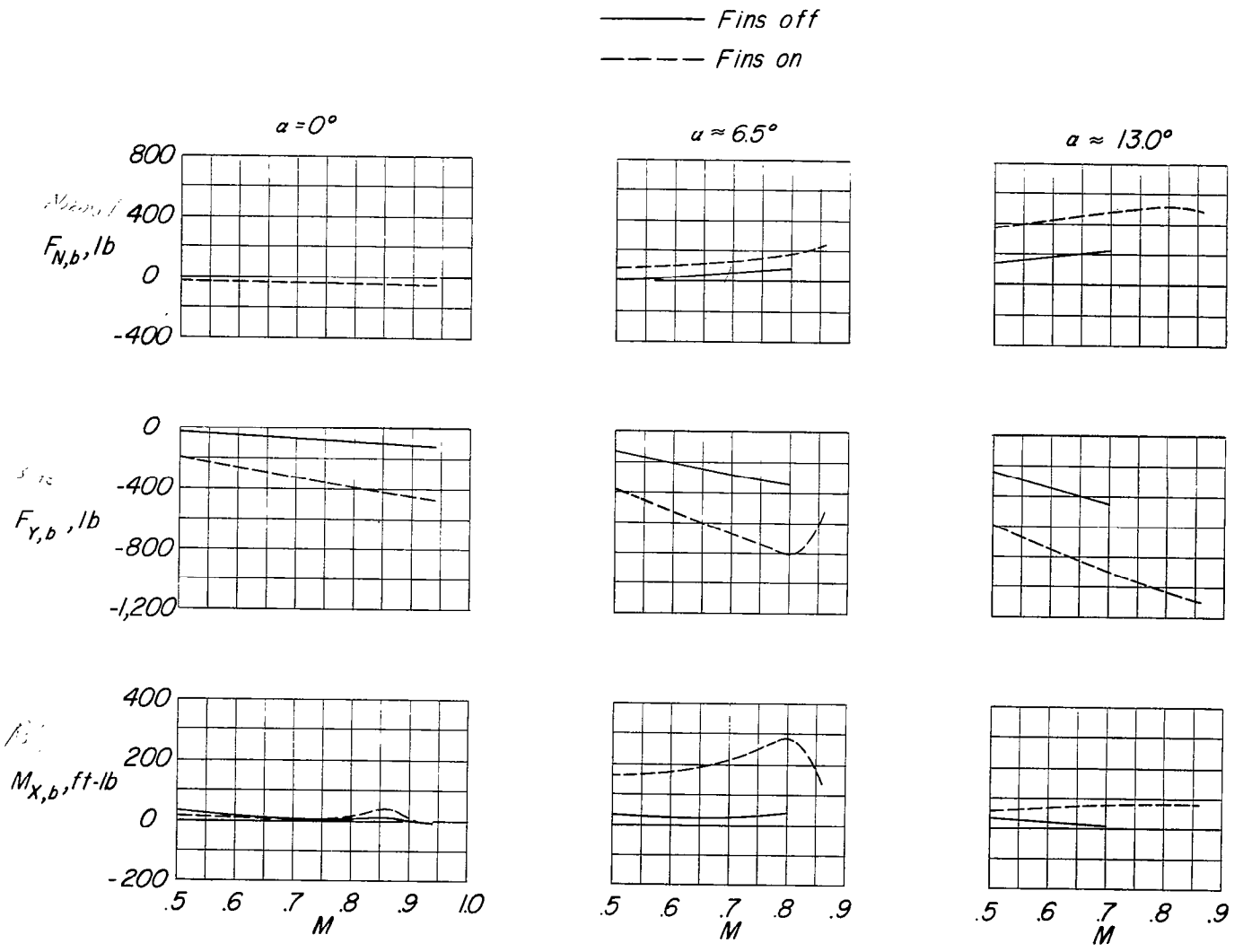

Figure 12.- Variation with Mach number of the loads on a body on the left wing tip of a hypothetical airplane. Altitude = 40,000 feet; $\beta = 8^{\circ}$.

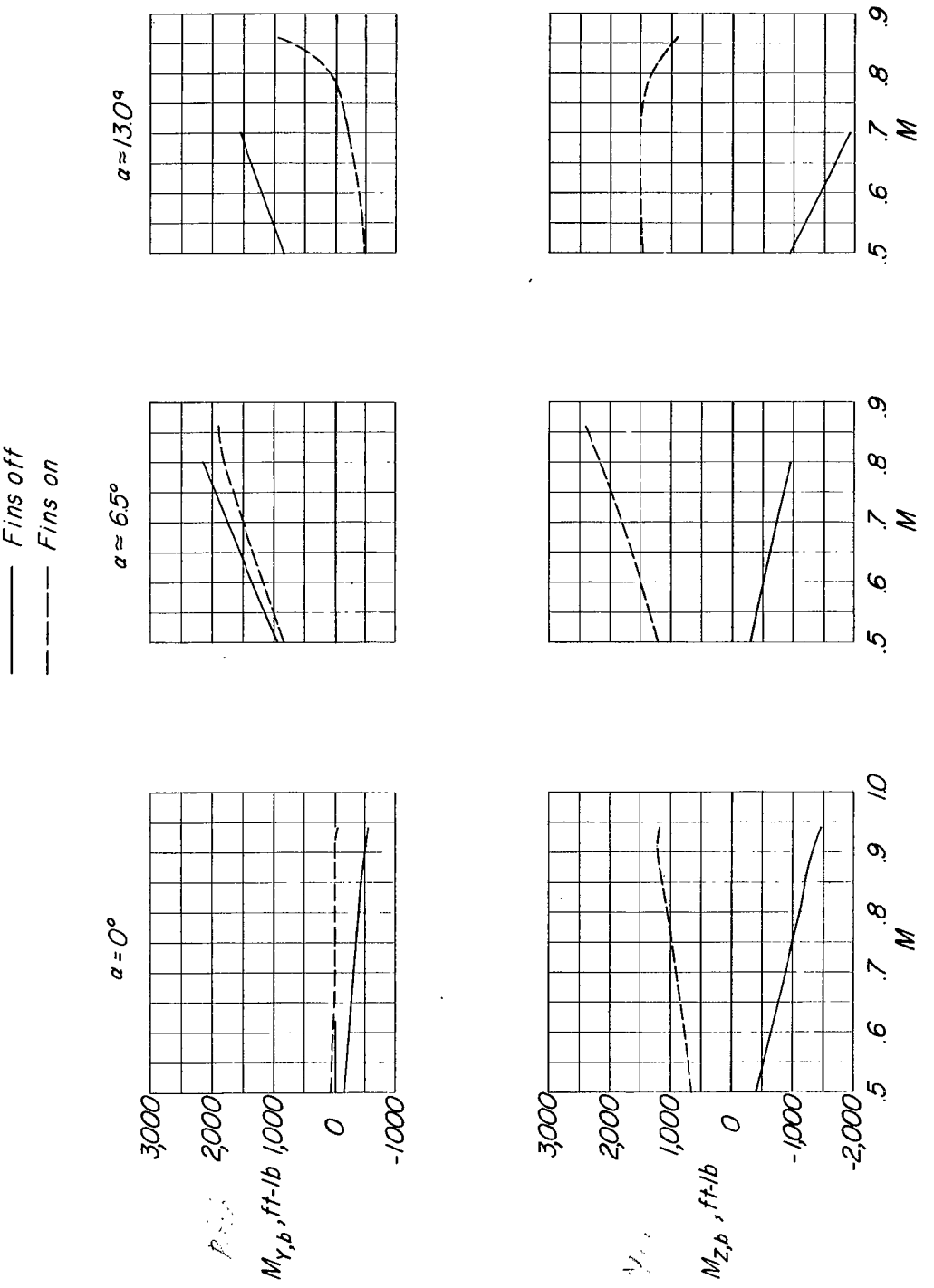

Figure 12.- Concluded.

NASA Technical Library
3 1176 01437 7668

CONFIDENTIAL